

A Fully Device-Independent Ternary Quantum Key Distribution Protocol Based on the Impossible Colouring Game

Aniket Basak^{1,*}, Rajeev Ghosh^{2,†}, Rohit Sarma Sarkar^{3,‡}, Chandan Goswami^{4,§} and Avishek Adhikari^{5,¶}

¹*Cryptology and Security Research Unit, Indian Statistical Institute Kolkata, Kolkata 700108, India*

²*Department of Mathematics, Indian Institute of Technology Madras, Chennai 600036, India*

³*Universitat Politècnica de Catalunya, Barcelona 08034, Spain*

⁴*Department of Mathematics, Indian Institute of Technology Kharagpur, Kharagpur 721302, India and*

⁵*Department of Mathematics, Presidency University, Kolkata 700073, India*

We propose a Ternary Fully Device-Independent Quantum Key Distribution (TFDIQKD) protocol based on the two-party Impossible Colouring pseudo-telepathy game, utilizing maximally entangled qutrit states to enable secure key generation between distant parties. The protocol harnesses Bell inequality violations that arise from contextuality in the Kochen-Specker theorem, thereby offering a quantum advantage in a task that is classically impossible and eliminating reliance on assumptions about the internal functioning of quantum devices. A specially designed qutrit quantum circuit is used for state preparation. Security and device independence are rigorously analyzed within a composable framework, employing Bell-inequality violations, smooth min-entropy, von Neumann entropy, and Shannon entropy. The protocol achieves optimal key rates in the ideal case and maintains security under significant noise, with a finite-key analysis that supports its practical viability. Overall, the protocol operates within an adequate security framework and demonstrates an improved key generation rate compared to standard quantum key distribution schemes, highlighting the potential of high-dimensional quantum systems for secure communication.

Keywords. Pseudo Telepathy Game, Kochen-Specker Theorem, Impossible Colouring Game, Fully Device-Independent Quantum Key Distribution, Maximally Qutrit Entangled State, Quantum Circuit

I. INTRODUCTION

Quantum Key Distribution (QKD) [1–3] is a secure communication protocol utilising the fundamental principles of quantum mechanics. It has emerged as a crucial solution, enabling two remote parties to establish a shared, secret key with information-theoretic security. In other words, this guarantees unconditional security based on the fundamental laws of quantum mechanics, making cryptographic protocols immune to attacks regardless of an adversary’s computational power. The need for QKD stems from the vulnerability that quantum computers pose to classical cryptographic systems. While some symmetric key ciphers remain resistant to quantum attacks, particularly against Grover’s search [4] and counting algorithms [5], the traditional approach of using public-key cryptography to share symmetric keys is

now vulnerable. In order to address this challenge, two approaches have surfaced in literature. The first involves designing classical post-quantum cryptographic schemes based on quantum-resistant hardness assumptions. While these systems offer strong security, they often introduce computational overhead, particularly in signature schemes and bandwidth usage, though they remain practical for real-world deployment. The second approach is to utilize the inherent hardness of quantum mechanics in order to create an unconditionally secure key for communication over public channels and to protect against both classical and quantum attacks. This quantum approach primarily relies on two fundamental principles, viz. the security provided by quantum measurement and the security derived from quantum entanglement.

The security of QKD relies on the no-cloning theorem [6] and quantum measurement-induced disturbance, ensuring that any eavesdropping attempt alters the quantum state, making interception detectable. QKD offers the advantage of generating fresh, secure cryptographic keys that can be immediately utilized. In order to achieve this, a significant final key must be generated in a very short time frame. A significant benefit of QKD is that, since communication is quantum, an adversary does not retain a classical transcript once a QKD session concludes. The fundamental steps of QKD protocols include quantum state distribution, parameter estimation, block-wise measurement, and classical postprocessing. The concept of QKD was first introduced by

* ¹ aniket2001basak@gmail.com

† ² rajeev.ghosh@students.iiserpune.ac.in

‡ ⁴ rohit15sarkar@yahoo.com (Corresponding Author)

§ ³ 7cgoswami@gmail.com

¶ ⁵ avishek.adh@gmail.com

Bennett and Brassard in 1984 with their BB84 protocol [2]. Since then, numerous modifications, extensions, and variants have been proposed [1, 7–11]. In 1991, Ekert [12] introduced the first entanglement-based QKD protocol. The security of these protocols fundamentally relies on the assumption that the communicating parties use either single-photon sources or maximally entangled states. However, conventional QKD protocols, such as BB84, face challenges in practical implementation due to factors like noise and limited key rates. To overcome these limitations, Device-Independent Quantum Key Distribution (DIQKD) has gained prominence, offering security guarantees without assumptions about the internal workings of quantum devices. DIQKD protocols typically rely on Bell non-locality tests, but their efficiency is often constrained by low key rates.

In DIQKD [13, 14], two honest parties at remote locations aim to establish a secure cryptographic key. Unlike traditional key distribution protocols, the security of a QKD is based on the fundamental principles of quantum mechanics. For DIQKD, in particular, the emphasis is on reducing trust in the internal working of the devices utilized by the communication parties. Rather than assuming optimal implementation, DIQKD protocols derive security directly from observable statistics, frequently by testing for non-classical correlations that signal the presence of quantum entanglement or system dimension limitations. This design allows key distribution even when devices are imperfect or partially untrusted. In this paradigm, all devices involved in preparing, transmitting, and measuring information carriers are treated as black boxes, meaning they could have been created or manipulated by an adversary. This ensures security even when the internal workings of the devices are unknown or potentially compromised. It is to be noted that, despite its name, DIQKD can still assume some level of trust in certain components. For example, Measurement-Device-Independent QKD (MDI-QKD) assumes trusted state preparation but removes trust from the measurement devices. The fundamental requirement is that the two honest parties remain spatially separated to prevent hidden communication between their devices. Other works like memory-assisted MDI-QKD protocols [15] in literature.

There also exist versions of DIQKD, known as fully DIQKD (FDIQKD) [16], where one eliminates any trust in all quantum devices, including the source and preparation of quantum states, which could potentially be adversarially controlled. In this paradigm, the only assumption on the devices is that they can be modeled by the laws of quantum mechanics, and that they are spatially isolated from each other and from any adversary’s laboratory. Also, the devices may have quantum memory [17]. FDIQKD ensures

security purely from the violation of Bell inequalities [18, 19]. It is considered to be the strongest form of device-independent key distribution. While DIQKD in general and FDIQKD in particular rely on spatial separation and quantum correlations, the latter provides stronger security guarantees by removing even minimal trust in state preparation through the use of Bell inequalities.

However, this increased security comes with greater experimental challenges, making FDIQKD more difficult to implement in practice [16, 17]. FDIQKD requires sources of quantum states that are completely untrusted, meaning security must be established purely through Bell inequality violations. This is extremely challenging because state preparation is often imperfect in real-world implementations [16, 17]. In contrast, protocols that relax these assumptions, such as those allowing partial trust in device components or those using dimension-based constraints, offer more practical implementations but at the cost of reduced security. These variants serve as intermediate steps but do not achieve the same level of device independence as FDIQKD.

Moreover, FDIQKD is not constrained by dimension assumptions or detailed device models, ensuring that its security proofs approach the theoretical optimum dictated by quantum mechanics [16, 17]. By closing all detection-related loopholes, it offers foolproof security against increasingly sophisticated attacks [20, 21]. While current technology still faces hurdles in terms of detection efficiency and channel losses, rapid advances in quantum hardware are steadily reducing these limitations. Thus, FDIQKD stands as the most secure paradigm available today, and continued progress in experimental platforms is expected to make it increasingly practical for real-world deployment [22].

Thus, in this work, we propose a Ternary FDIQKD (TFDIQKD) protocol based on the Impossible Colouring pseudo-telepathy game [23]. By employing an appropriate quantum strategy, both parties can achieve a unit probability of winning, surpassing the success rate of other non-local games such as the CHSH game [24]. In this theoretical framework, we introduce a novel approach to enhancing both security and efficiency in quantum cryptography. Unlike conventional qubit-based QKD schemes, our protocol operates on qutrits (three-level quantum systems), which offer sending of larger information for a given transmission in a channel [25], improved noise resilience [26, 27], and stronger security [25] due to more complex quantum correlations. Also, the implementation is feasible through the use of angular momentum modes [28] or time bins [29][30]. They have also been generated using bipho-

tons, as shown by Bogdanov et al. [31]. The Impossible Colouring Game serves as the foundation of our protocol. This provides a unit quantum-winning probability while being classically unwinnable, which points to an inherently secure key exchange. There already exist several DIQKD protocols using qutrits [19, 32–34]. However, our proposed Ternary Fully Device-Independent Quantum Key Distribution is a novel implementation of QKD using a qutrit-based pseudo-telepathy game, significantly advancing the security and efficiency of quantum cryptographic systems. We also establish the security of our protocol through a rigorous analysis based on smooth minimum entropy, von Neumann entropy, and Shannon entropy, demonstrating its robustness against quantum attacks. It is of note that, unlike the binary system of classical computers, superconducting qubits [35] and trapped-ion quantum computers [36] theoretically possess discrete energy levels spanning an infinite spectrum, making them naturally suited for qudit-based computations. Further, qutrits (or qudits), contrary to their classical counterpart known as the ternary bits (or trits), can be realistically generated and store more information than qubits. While numerous quantum walk experiments have been conducted on real quantum hardware using qubits [35–39], efficiently implementing similar experiments with qutrits and higher-dimensional qudits remains a significant challenge [40]. Nonetheless, qutrit-based circuit models have garnered substantial interest as an alternative to qubit circuits due to their potential for resource-efficient computation [41, 42]. Recent advancements in hybrid quantum circuits suggest that incorporating intermediate qutrits instead of qubits enables more efficient decomposition of n -qubit unitary gates [41, 43]. Notably, qutrit-based synthesis has demonstrated logarithmic depth reductions, leading to an exponential decrease in resource requirements. Specifically, qutrit circuits require 70 times fewer two-qudit gates compared to conventional two-qubit (CNOT) gates. Furthermore, qutrit-based processors have been theoretically shown to enhance quantum error correction with smaller code sizes [44, 45] and play a pivotal role in high-fidelity magic state distillation [46], robust quantum cryptography [47, 48], and secure quantum communication protocols [49]. Recent benchmarking efforts on a five-qutrit processor have reported remarkably low single-qutrit gate infidelity [50], indicating promising advancements toward practical qutrit-based computation. Literature also exists on quantum walk circuit constructions [51], including qutrit circuits designed for three-state lazy quantum walks on a line [52] and qudit circuits for d -state discrete-time quantum walks (DTQWs) on a lattice [53]. Further, the generalization of quantum algo-

rithms—such as Shor’s algorithm and the Deutsch-Josza algorithm—to qutrit systems has been explored [54–56]. A particularly notable development is the recent formulation of the Quantum Approximate Optimization Algorithm (QAOA) for solving the graph 3-coloring problem using qutrits, which significantly reduces circuit depth and entangling gate count per layer [57]. Moreover, methods for synthesizing qudit gates have been detailed in [58], further enriching the foundation for scalable quantum computing using qutrits and higher-dimensional qudits. In [59], the authors also provided a scalable qutrit circuit model for simulating discrete-time quantum walks on Cayley graphs of dihedral groups. Qutrits also offer superior security compared to qubit-based QKD, as their higher-dimensional quantum correlations enhance resilience against adversarial attacks.

Despite the current challenges in constructing qutrit-based QKD systems, primarily due to technological constraints, our approach establishes a strong theoretical foundation for future implementations. A fundamental challenge that is present is the lack of well-established simulation frameworks for qutrit-based systems, making practical verification uncertain at present. Although platforms like Google Cirq [60] allow for qutrit computations, a lot of gates have to be defined manually at the start of the program, making the endeavour quite cumbersome. However, recent developments of Google’s Cirq framework supporting qudit-based computations suggest that the feasibility of qutrit-based QKD simulations may soon become a reality, opening new avenues for experimental validation.

One of the key advantages of QKD is the ability to generate fresh, secure keys in real-time, allowing immediate utilization for secure communication. Achieving this requires a significant final key generation rate within a matter of seconds. Our protocol achieves the highest key rate among existing DIQKD protocols while maintaining optimal bit wastage and significantly improved noise tolerance. Specifically, we show that our protocol achieves a higher key rate (see Section IV D) than even the BB84 protocol [2], particularly in the ideal case of zero noise. Subsequently, we generalize Renner et. al’s [61] qubit-based key rate formula for one-way QKD protocols, extending its applicability to qutrit systems. The proposed protocol works on a maximally entangled qutrit state, enabling more efficient information encoding, increased computational complexity, and greater robustness [34] against any variants of noise. Since employing higher-dimensional systems enhances the security of QKD protocols by introducing more complex correlations that are more difficult for an eavesdropper to exploit, the qutrit-based protocol also helps in enhancing the security of QKD

protocols by generating more intricate correlations that are difficult for an eavesdropper to intercept, while simultaneously enabling higher key rates.

We also demonstrate that our protocol is ϵ -correct (Definition IV.1). If an eavesdropper has a strong correlation with the system shared by the two parties, this can be detected during the testing phase. The successful completion of this phase ensures that there is no (or negligible) correlation, thus affirming the DIQKD protocol's efficacy. Moreover, the output of our proposed protocol, i.e., the raw key, is at most η -distinguishable (Definition IV.6). We have also validated the security of our proposed scheme, utilizing the special case of the Impossible Colouring game described in section II through the state-of-the-art security framework proposed by Renner [61, 62] and also used by Xu et al. [63] and Tomamichel et al. [64]. In fact, the security analysis of our protocol follows the standard theoretical proof, which is based on the concepts of smooth minimum-entropy, von Neumann entropy, and binary Shannon entropy [5]. Furthermore, we have also carried out a finite-key analysis for the same.

Our proposed protocol also outperforms existing DIQKD protocols and exhibits significantly high noise tolerance. Moreover, we also establish that our key rate remains independent of the number of input subsystems, making it constant regardless of the choice of input subsystems. For a comparative performance analysis of our protocol with other state-of-the-art DIQKD protocols, see Table IV.

The paper is organized as follows. In Section II, we introduce the basic structure of generic device-independent quantum key distribution protocols, followed by a discussion of the two-party impossible coloring game in Section II A. In Section III, we present our proposed device-independent quantum key distribution protocol. An illustrative example is provided in Section III A, and the complete protocol, along with the raw key generation procedure using maximally entangled states, is detailed in Section III B. Section III C describes the quantum circuit construction required for preparing maximally entangled qutrit Bell states. Section IV presents the security analysis, including correctness, device independence, and the security of both the raw and active keys. The paper concludes in Section V.

II. PRELIMINARIES

In this section, we shall provide background on the two-party impossible coloring game, the generic DIQKD protocol, and other fundamental aspects of the protocol that will be used in the later part of the paper.

Firstly, we shall take a look at the history of DIQKD protocols. In 2014, Vazirani et al.[17] introduced a device-independent quantum Key Distribution (DIQKD) protocol based on the Clauser-Horne-Shimony-Holt (CHSH) game[24] to certify the maximality of entanglement. Later, in 2019, Basak et al.[65] and, in 2023, Zhen et al.[14] proposed two DIQKD protocols utilizing the Parity game [23] and the Mermin-Peres Magic Square game [66], respectively. Both of these games have a unit probability of being won using a quantum strategy (compared to 0.85 in CHSH) and their protocols have been shown to be secure as well. Furthermore, these protocols allow key generation using a single measurement basis, unlike the VVQKD (Vazirani-Vidick Quantum Key Distribution) protocol[16, 17]. However, the key rate in these DIQKD protocols remains low because it depends on the number of subsystems involved in the measurement process. When fewer subsystems are used, the key rate decreases. Further, the games used in these protocols can be won with some probability using classical strategies, making them susceptible to classical attacks. To address these limitations, we propose a DIQKD protocol based on the Impossible Colouring game, which offers improved security and key generation efficiency.

In Figure 1, following the footsteps of [61, 67], we depict a schematic diagram representation of a generic DIQKD protocol.

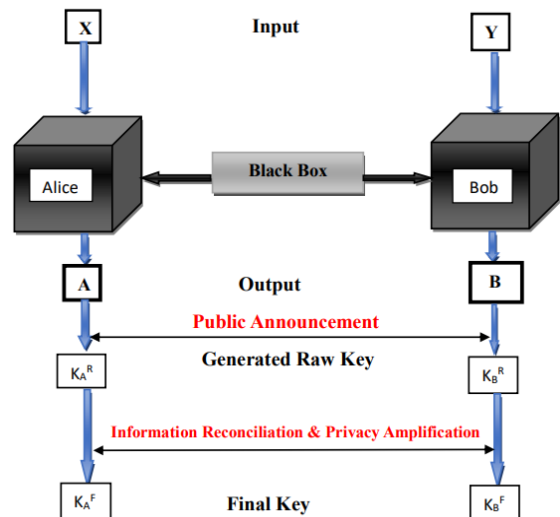


Figure 1: Generic DIQKD Protocol.

The road-map in Figure 1 depicts that after raw Key Distribution, the process must proceed through parameter estimation, blockwise measurement, information reconciliation, and privacy amplification to generate the final shared secret key securely. We re-

call that parameter estimation protocol is a two-party procedure in which Alice and Bob, upon receiving inputs from respective Hilbert spaces, perform measurements or computations to estimate certain parameters of the shared system, and based on the estimated values, either output accept or abort the protocol. Information reconciliation is the process by which two parties with similar but imperfectly correlated data communicate in order to correct discrepancies and agree on a common value without revealing the original data. In this context, Alice retains her input x , while Bob, holding a correlated input, uses communication to produce an output x' that matches Alice's value as closely as possible. Privacy amplification is a fundamental technique for extracting a secure key from a partially secret string. It involves applying a randomly chosen hash function from a two-universal family to the input. The resulting key is provably secure, provided that its length is less than the adversary's uncertainty about the input, as quantified by the (smooth) minimum-entropy.

The Impossible Colouring game [23] is a special type of non-local game in which a quantum strategy enables two players to win with unit probability, while winning with certainty is impossible using classical strategies. Typically, two communicating parties perform a non-locality test [68] to assess the extent of an adversary's potential knowledge about the generated data. The results of this test are then used to decide whether the data is suitable for generating secure keys [13, 69]. A detailed description of the two-party Impossible Colouring game is provided in the next section.

A. Two Party Impossible Colouring Game

In this section, we describe the Impossible Colouring game, which forms the central idea behind our proposed DIQKD protocol. In order to understand the Impossible Colouring game [23], it is necessary to first be familiar with the Kochen-Specker theorem [70].

Theorem II.1 ([70]). *In $\mathbb{R}^d (d \geq 3)$, there is a finite and explicit set of vectors that cannot be $\{0, 1\}$ -coloured, such that the two following criteria hold simultaneously.*

- i. *For every orthogonal pair of vectors, at most one is coloured 1*
- ii. *For every mutually orthogonal triple of vectors, at least one of them and therefore exactly one is coloured 1.*

In order to explain Theorem II.1 and subsequently establish our results, we consider the following. Let

V denote the subset of vectors in \mathbb{R}^d ($d \geq 3$) that satisfy the conditions of the Kochen-Specker theorem (Theorem II.1).

In the Impossible Colouring game [23], Alice receives a mutually orthogonal d -tuple of vectors v_1, v_2, \dots, v_d , where all vectors are elements of V . Bob, on the other hand, receives a single vector v_ℓ , which is also taken from V . The promise of the game is that v_ℓ is always one of the vectors given to Alice. They color the vectors as $\{0, 1\}$ which fulfills the following criteria:

- i. Any two orthogonal vectors in V are not both coloured 1
- ii. Exactly one of Alice's vectors is coloured 1 if she is given d vectors
- iii. Alice and Bob assign the same colour to the vector v_ℓ .

In order to meet the aforementioned requirements, if Alice is given d vectors, she should produce $a \in \{1, 2, \dots, d\}$ as her output, indicating that color 1 should be assigned to the vector v_a . Similarly, Bob, upon receiving his input, outputs a single bit b corresponding to the color assigned to the vector v_ℓ . To win the game, it is necessary that both Alice and Bob assign the same color to v_ℓ .

Here, no communication is allowed among the participants after receiving their respective inputs and before producing their outputs. It has been proved in [23] that there does not exist any classical winning strategy for this game. However, quantum entanglement provides an advantage as it has been shown that there exists a perfect quantum strategy by which both parties can always win the game [23].

While describing the quantum winning strategy for this game, let us define the necessary shared entangled state as

$$|\psi\rangle = \frac{1}{\sqrt{d}} \sum_{j=0}^{d-1} |j\rangle |j\rangle \quad (1)$$

Both parties are allowed to share the aforementioned entangled state (Equation 1) prior to the start of the game. Upon receiving her input, Alice is given two orthogonal vectors v_1 and v_2 from the set V . She then selects $d - 2$ additional vectors, denoted by v_3, v_4, \dots, v_d , which are not necessarily elements of V , such that the set $\{v_1, v_2, \dots, v_d\}$ forms an orthogonal d -tuple. Subsequently, she performs a measurement on her share of the entangled state with respect to the basis B_a , which consists of these d vectors after proper orthonormalization, if necessary. Similarly, Bob receives a single vector v_ℓ and selects $d - 1$

additional vectors, again not necessarily from V , to complete an orthogonal d -tuple. He then performs a measurement on his share of the entangled state with respect to the corresponding orthonormal basis.

After performing their respective measurements, we consider the probability that Alice obtains the outcome corresponding to v_i ($i \in \{1, 2, \dots, d\}$) while Bob obtains the outcome corresponding to v_ℓ . By following suitable mathematical computations as outlined in [23], it can be shown that Bob measures v_ℓ if and only if Alice also measures v_ℓ . Consequently, Alice and Bob assign the same color to the vector they have received in common, allowing them to win the game with certainty, without any communication between them. For our proposed protocol, we consider the pseudo-telepathy game with $d = 3$, where $V = V^{\text{KS}}$ is a subset of \mathbb{R}^3 . Originally, Theorem II.1 was proved using 117 vectors [71]. Few modifications were done by reducing it to 37 vectors [72], 33 vectors [73, 74]. Later, Conway and Kochen reduced this to 31 vectors grouped into 17 orthogonal triples [70] which we have used in our construction.

In this work, we adhere to the fixed set of notations depicted in Table I. Any additional symbols will be introduced and explained as they appear in the relevant sections.

III. DESCRIPTION OF PROPOSED TFDIQKD PROTOCOL

Alice and Bob aim to communicate over a potentially insecure channel to which an eavesdropper, Eve, may have access. To securely establish a shared secret key over such an unreliable or insecure chan-

nel, they require a QKD protocol. Ideally, the key should be generated without relying on trusted devices. Furthermore, they seek to generate a shared secret key that is classically impossible to compromise and achieves a sufficiently high key rate. These considerations motivate the development of the DIQKD protocol proposed in this work.

In our proposed DIQKD protocol, we assume that Alice and Bob each possess three black boxes, denoted by D_1^A, D_2^A, D_3^A for Alice and D_1^B, D_2^B, D_3^B for Bob, respectively. The first two black boxes of Alice accept inputs $|v_1\rangle$ and $|v_2\rangle$, where $v_1, v_2 \in V^{\text{KS}}$ (a subset of \mathbb{R}^3 satisfying the Kochen-Specker property), such that $|v_1\rangle$ and $|v_2\rangle$ are orthogonal. The remaining black box of Alice accepts as input a vector $|v_a\rangle$, where v_a is any vector in \mathbb{R}^3 (not necessarily from V^{KS}), such that $|v_a\rangle$ is orthogonal to both $|v_1\rangle$ and $|v_2\rangle$.

Alice sends the first two vectors selected from V^{KS} to Bob one by one through a public channel, which is assumed to be accessible to Eve. Before starting the game, Alice informs Bob which of the received vectors corresponds to $|v_1\rangle$ and which corresponds to $|v_2\rangle$, which ensures that Bob selects his measurement basis correctly.

Subsequently, Bob randomly selects one of the vectors received from Alice as the input for his first black-box (D_1^B), denoted by $|v_\ell\rangle$. The other two black boxes accept inputs $|v_{b_1}\rangle$ and $|v_{b_2}\rangle$, where v_{b_1} and v_{b_2} are vectors in \mathbb{R}^3 (not necessarily elements of V^{KS}) that are orthogonal to v_ℓ . We assume that the devices, as in previous device-independent QKD protocols [14, 16, 65], operate according to the principles of quantum mechanics and are physically isolated from one another as well as from any potential adversaries.

Symbols	Descriptions
V	subset of vectors of \mathbb{R}^d which satisfies Kochen-Specker theorem
V^{KS}	subset of vectors of \mathbb{R}^3 which satisfies Kochen-Specker theorem
$h(\kappa)$	ternary Shannon entropy with bias κ
$H(P_X)$	Shannon entropy of the probability distribution P_X
$\epsilon_{correct}$	correct except with probability ϵ
ϵ_{secure}	secure except with probability ϵ
η	noise tolerance
l	length of the active key generated after privacy amplification
\mathcal{N}	number of input systems
p	number of subsystems that are sacrificed for parameter estimation
q	size of each block
n	number of blocks of size q that are used for the actual computation of the key
$H(\rho_A)$	Von Neumann entropy of the density operator ρ_A
$H(A B)$	conditional entropy $H(\rho_{AB}) - H(\rho_B)$
H_{min}^ϵ	smooth minimum-entropy measures for density operator
H_{max}^ϵ	smooth maximum-entropy measures for density operator
r	key rate
c	tunable parameter

Table I: Overview of notations.

Prior to the protocol's initiation, we assume that Alice and Bob receive \mathcal{N} copies of qutrit entangled states $\frac{1}{\sqrt{3}}(|00\rangle + |11\rangle + |22\rangle)$ that are supplied by a third party. The quantum circuit for the preparation of such a state, along with some background on qutrit circuits, is provided in Section III C.

At this stage, Alice and Bob begin their respective measurement procedures, during which communication between them is strictly prohibited. Upon receiving their inputs, Alice performs a measurement on her share of the entangled state in the basis $B_a = \{|v_1\rangle, |v_2\rangle, |v_a\rangle\} \subset \mathbb{R}^3$, where orthonormalization is applied if necessary. Similarly, Bob measures his share of the entangled state in the basis $B_b = \{|v_\ell\rangle, |v_{b_1}\rangle, |v_{b_2}\rangle\} \subset \mathbb{R}^3$, also applying orthonormalization if required.

After performing the measurement, Bob publicly announces his output. He declares 0 if the outcome corresponds to $|v_\ell\rangle$ and 1 otherwise. According to the quantum winning strategy for the Impossible Colouring game [23], Bob obtains $|v_\ell\rangle$ as an outcome if and only if Alice also obtains $|v_\ell\rangle$. Thus, if Bob declares 0, Alice can infer the chosen vector $|v_\ell\rangle$, and if he declares 1, the round is discarded.

After the measurement phase, Alice and Bob discard all instances where Bob did not measure the vector $|v_\ell\rangle$. As a result, approximately $\frac{2\mathcal{N}}{3}$ of the total inputs are discarded. Let the remaining set of

rounds be denoted by \mathcal{A} . They then randomly select a subset of size $\gamma|\mathcal{A}|$, with $0 < \gamma < 1$, to estimate the success probability of the protocol by checking how often the Impossible Colouring game condition is satisfied. If the observed success probability falls below the threshold $(1 - \eta)$, where η represents the acceptable noise level, the protocol is aborted. Otherwise, they proceed to generate a shared secret key using the remaining $(1 - \gamma)|\mathcal{A}|$ rounds.

In the key extraction phase, if Bob selects $|v_\ell\rangle = |v_1\rangle$, both Alice and Bob output 0, thereby assigning the shared bit value 0. Similarly, if Bob chooses $|v_\ell\rangle = |v_2\rangle$, both parties output 1, resulting in the shared bit value 1. In this way, the raw key is generated from the outcomes of the successful rounds.

Following the raw key generation, both parties perform classical post-processing, which consists of two main steps: information reconciliation and privacy amplification. During the information reconciliation phase, Alice and Bob exchange information over a public authenticated channel to identify and correct discrepancies in their respective keys. Typically, this involves performing parity checks on short blocks obtained by partitioning the raw key string. As a result, they obtain identical but partially compromised keys. In the subsequent privacy amplification step, they apply a suitable technique, such as a universal hash function or syndrome decoding, to compress the rec-

onciled key into a shorter final key. This final key has significantly reduced information leakage, thereby ensuring that any potential information available to an eavesdropper is rendered negligible. We illustrate our proposed TFDIQKD protocol through an example provided in the next Section III A.

A. Example

Let Alice and Bob want to generate an 8-bit shared secret key. To do this, as explained in the protocol description, Alice and Bob require approximately 24 entangled states, with $|v_\ell\rangle$ measured on Bob's side in roughly $24/3 = 8$ times. Probabilistically, $|v_\ell\rangle$ will not be measured 16 times, so we need to discard approximately 16 rounds; the remaining 8 rounds will provide us desired secret key for both parties. Without loss of generality assume that Bob measures $|v_\ell\rangle = |v_1\rangle$ in rounds 2, 3, 4, and 8, and $|v_2\rangle$ in the others. By the properties of the Impossible Colouring game described before and in Algorithm 2, their outputs match in each valid round, producing the raw key 10001110.

Due to noise, discrepancies may arise. For instance, Bob may obtain 10000110. To correct this, they perform information reconciliation by dividing the key into blocks (e.g., 4 bits) and comparing parities. If a mismatch is detected, the block is split to two sub-blocks and so on to locate the error. For example, Alice's last block may have parity $1 \oplus 1 \oplus 1 \oplus 0 = 1$ (odd), while Bob's is $0 \oplus 1 \oplus 1 \oplus 0 = 0$ (even). Therefore, they will split further into 2 length blocks.

After this step, Alice and Bob obtain identical but potentially partially compromised keys. For example, the parities of a block may match even if their bits differ, such as Alice having 1111 and Bob 0011. To reduce information leakage, they perform privacy amplification by applying syndrome decoding or a universal hash function, yielding a shorter, secure key. The final key reveals negligible information to any eavesdropper.

B. Algorithm of TFDIQKD protocol

This section presents the DIQKD protocol based on the Impossible Colouring game. Algorithm 1 describes raw key generation and the subsequent classical post-processing to obtain the final key.

Algorithm 1 Proposed TFDIQKD Protocol using Impossible Colouring Game

Input: \mathcal{N} many entangled states $\frac{1}{\sqrt{3}}(|00\rangle + |11\rangle + |22\rangle)$ and noise tolerance η

Output: Shared common keystream

Procedure:

1. State Preparation:

- Alice selects $|v_1\rangle, |v_2\rangle$ from V^{KS} such that they are orthogonal and inputs them into her first two blackboxes. The remaining blackbox of Alice takes $|v_a\rangle$, any vector of \mathbb{R}^3 (not necessarily from V^{KS}) as input, which is orthogonal to both $|v_1\rangle$ and $|v_2\rangle$.
- Alice sends the first two vectors selected from V^{KS} to Bob one by one through a secure channel. According to their strategy, the first vector received by Bob is $|v_1\rangle$, and $|v_2\rangle$ will be the next.
- Bob chooses randomly one vector received from Alice $|v_\ell\rangle$ as input for the first black box and the other two black boxes take $|v_{b_1}\rangle, |v_{b_2}\rangle$ from \mathbb{R}^3 , which is perpendicular to $|v_\ell\rangle$.

2. Measurement: Alice measures her share of the entangled state in basis $B_a = \{|v_1\rangle, |v_2\rangle, |v_a\rangle\}$ after orthonormalization and similarly, Bob measures on his share of the entangled state in basis $B_b = \{|v_\ell\rangle, |v_{b_1}\rangle, |v_{b_2}\rangle\}$ of \mathbb{R}^3 performing necessary normalization.

3. Announcement: Bob declares his output publicly 0 if $|v_\ell\rangle$ measure and 1 otherwise. Because of the quantum strategy, when Bob declares 0, then by observing his output, Alice can surely understand what $|v_\ell\rangle$ was chosen by Bob. If Bob declares 1 as output, then they will discard the step. Let the set \mathcal{A} contain all those cases that are not discarded.

4. Testing: Alice chooses a random subset $\mathcal{B} \subseteq \mathcal{A}$ of size $\gamma|\mathcal{A}|$ where $0 < \gamma \leq 1$. After measuring the outputs, they discuss their inputs and outputs publicly and estimate the left-hand side of the Bell inequality as mentioned in Equation 5, over $\mathcal{A} \setminus \mathcal{B}$. If this inequality is true, then they abort the protocol. Otherwise, they continue the process for \mathcal{B} .

5. Key Extraction: In \mathcal{A} , when Bob chooses $|v_\ell\rangle$ as $|v_1\rangle$, after measurement Bob gives output 0 and simultaneously Alice will give output 0, so their shared common bit becomes 0, and when Bob chooses $|v_\ell\rangle$ as $|v_2\rangle$, similarly the bit string will be 1. Hence, the raw key will be generated.

6. Classical Post Processing: After the generation of the raw key, Alice and Bob will perform Information Reconciliation and Privacy Amplification to generate the final key with negligible information leakage to ensure that Eve hardly knows anything about it.

Algorithm 1 describes the process of raw key gen-

eration and the subsequent classical post-processing to obtain the final key in our proposed DIQKD protocol, which is based on the Impossible Colouring game. Initially, the raw key is generated by Alice and Bob performing quantum measurements based on the pre-shared entangled state and the Impossible Colouring game. The measurement results, denoted as m_A and m_B , are then used to construct the raw key. A Bell test is applied to verify the violation of Bell's inequality, ensuring the device-independent nature of the protocol. After discarding inconsistent results that do not satisfy the Bell test, classical post-processing steps, such as error correction and privacy amplification, are applied to the raw key. The final outcome is a secure, shared secret key between Alice and Bob.

In Figure 1, we depicted the pseudocode for the generic QKD protocol, where the most crucial step was Raw Key generation. The raw key generation was done using a qutrit entangled state and the pseudocode for the same is depicted in Algorithm 2.

Algorithm 2 Qutrit Entanglement-based Raw Key Distribution

Require:

- \mathcal{N} -many entangled state $|\psi\rangle = \frac{1}{\sqrt{3}}(|00\rangle + |11\rangle + |22\rangle)$
[Bases for encoding]
- Noise tolerance = η

Ensure: Raw key without involvement of any devices

function ENTANGLEMENT BASED RAWKEYDISTRIBUTION

$i=1$

while $i \leq \mathcal{N}$ **do**

Alice chooses $B_a = \{|v_1\rangle, |v_2\rangle, |v_a\rangle\}$

Bob chooses $B_b = \{|v_\ell\rangle, |v_{b_1}\rangle, |v_{b_2}\rangle\}$, with $v_\ell \stackrel{\S}{\leftarrow} \{v_1, v_2\}$

Alice and Bob measure using their basis

if $|v_\ell\rangle$ not measured **then**
return (\perp, \perp) and **discard**

if $|v_\ell\rangle$ is $|v_1\rangle$ **then**
return 0

if $|v_\ell\rangle$ is $|v_2\rangle$ **then**
return 1

$i := i + 1$

return $(\mathbf{K}_A^R, \mathbf{K}_B^R)$

We shall now provide the quantum circuit which is required to construct the entangled state $\frac{|00\rangle+|11\rangle+|22\rangle}{\sqrt{3}}$ and other similar states also known as 3-dimensional Bell basis states [75].

C. Quantum circuits for preparation of ternary Bell basis

In this section, we design qutrit quantum circuits that prepare the maximally entangled states like $|\varphi_0\rangle = \frac{|00\rangle+|11\rangle+|22\rangle}{\sqrt{3}}$, which serves as a fundamental resource for our protocol. This state is an element of the 3-dimensional Bell basis, a natural generalization of the standard Bell basis to qutrit systems [75]. The complete 3-dimensional Bell basis is defined as follows:

$$\begin{aligned} |\varphi_0\rangle &= \frac{|00\rangle+|11\rangle+|22\rangle}{\sqrt{3}}, \\ |\varphi_1\rangle &= \frac{|00\rangle+\omega|11\rangle+\omega^2|22\rangle}{\sqrt{3}}, \\ |\varphi_2\rangle &= \frac{|00\rangle+\omega^2|11\rangle+\omega|22\rangle}{\sqrt{3}}, \\ |\varphi_3\rangle &= \frac{|01\rangle+|12\rangle+|20\rangle}{\sqrt{3}}, \\ |\varphi_4\rangle &= \frac{|01\rangle+\omega|12\rangle+\omega^2|20\rangle}{\sqrt{3}}, \\ |\varphi_5\rangle &= \frac{|01\rangle+\omega^2|12\rangle+\omega|20\rangle}{\sqrt{3}}, \\ |\varphi_6\rangle &= \frac{|02\rangle+|10\rangle+|21\rangle}{\sqrt{3}}, \\ |\varphi_7\rangle &= \frac{|02\rangle+\omega|10\rangle+\omega^2|21\rangle}{\sqrt{3}}, \\ |\varphi_8\rangle &= \frac{|02\rangle+\omega^2|10\rangle+\omega|21\rangle}{\sqrt{3}}. \end{aligned}$$

Here, $\omega = e^{2\pi i/3}$ is the principal cube root of unity. These states form an orthonormal basis for the joint qutrit Hilbert space $\mathbb{C}^3 \otimes \mathbb{C}^3$ and are frequently employed in high-dimensional entanglement-based quantum communication protocols. This set of maximally entangled two-qutrit states serves as the fundamental resource for implementing the quantum correlations required by our protocol. In order to construct a qutrit circuit for the preparation of the state, we shall discuss a bit about qutrit gates. From [59], we consider the following set of single qutrit gates

$$\begin{aligned} X_{0,1} &= \begin{bmatrix} 0 & 1 & 0 \\ 1 & 0 & 0 \\ 0 & 0 & 1 \end{bmatrix}, X_{1,2} = \begin{bmatrix} 1 & 0 & 0 \\ 0 & 0 & 1 \\ 0 & 1 & 0 \end{bmatrix}, \\ X_{0,2} &= \begin{bmatrix} 0 & 0 & 1 \\ 0 & 1 & 0 \\ 1 & 0 & 0 \end{bmatrix}, X_{+1} = \begin{bmatrix} 0 & 0 & 1 \\ 1 & 0 & 0 \\ 0 & 1 & 0 \end{bmatrix}, \\ X_{+2} &= \begin{bmatrix} 0 & 1 & 0 \\ 0 & 0 & 1 \\ 1 & 0 & 0 \end{bmatrix}. \end{aligned} \quad (2)$$

Obviously, the $X_{p,q}$ gate maps $|p\rangle_3$ (respectively, $|q\rangle_3$) to $|q\rangle_3$ (respectively, $|p\rangle_3$), where $p, q \in \{0, 1, 2\}$. The X_{+a} gate, on the other hand, defines a linear transformation from $|p\rangle_3$ to $|(a+p) \bmod 3\rangle_3$. We refer

to these single-qutrit gates collectively as *qutrit- X gates*, where $X \in \{X_{0,1}, X_{1,2}, X_{0,2}, X_{+1}, X_{+2}\}$. We also consider the single qutrit Hadamard gate [59]

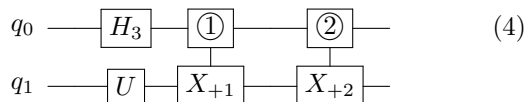
$$H_3 = \begin{bmatrix} 1 & 1 & 1 \\ 1 & \omega & \omega^2 \\ 1 & \omega^2 & \omega \end{bmatrix} \text{ where } \omega = \exp \frac{2\pi i}{3} \text{ i.e. a complex}$$

root of unity.

Also, following [59], we have the two-qutrit controlled- X gates represented by a quantum circuit given by



Obviously, this gate applies a one-qutrit X gate to the target (second) qutrit when the control (first) qutrit is in the state $\alpha \in \{0, 1, 2\}$. In particular, when $\alpha = 2$, such a gate is known as the Muthukrishnan–Stroud gate [76]. For further details on qutrit gates, see [59]. With this background, we shall construct a quantum circuit involving qutrits in order to prepare our 3-dimensional Bell states. Let us consider the following circuit.



It is straightforward to verify that if $U = I$ (the identity operator), then starting from the initial two-qutrit state $|00\rangle$ (i.e., $q_0 = q_1 = 0$), the output of the circuit is the maximally entangled state $|\varphi_0\rangle$. Similarly, if $U = X_{+1}$, the input $|00\rangle$ results in the output state $|\varphi_3\rangle$, and if $U = X_{+2}$, the output becomes $|\varphi_6\rangle$.

For the input $|10\rangle$, applying $U = I$ yields $|\varphi_1\rangle$, applying $U = X_{+1}$ gives $|\varphi_4\rangle$, and applying $U = X_{+2}$ produces $|\varphi_7\rangle$.

Finally, for the input $|20\rangle$, the circuit outputs $|\varphi_2\rangle$ when $U = I$, $|\varphi_5\rangle$ when $U = X_{+1}$, and $|\varphi_8\rangle$ when $U = X_{+2}$.

In the following section, we shall discuss the security analysis of our QKD protocol.

IV. SECURITY ANALYSIS OF OUR PROPOSED PROTOCOL

In this section, we shall exhibit the security of our QKD protocol. Although the characterization of the quantum state and the measurement devices is not required for the security of DIQKD, certain assumptions and security notions are still necessary to establish its security rigorously. The standard assumptions underlying the security analysis of our proposed protocols are outlined below.

i. **Memoryless Device:** The devices must operate in accordance with the principles of quantum mechanics, with each use being independent of previous uses, and must exhibit consistent behaviour across all trials.

ii. **Secured Laboratory:** Alice’s and Bob’s laboratories are assumed to be completely secure, preventing any leakage of confidential information. Furthermore, the laboratories are physically separated. This enables the modeling of their systems as jointly distributed quantum systems.

iii. **Random Seeds:** We assume that both parties have access to uniformly random seeds, which are typically generated locally using Quantum Random Number Generators (QRNGs) [77] within their respective laboratories.

iv. **Authenticated Communication Channel:** It is assumed that Alice and Bob communicate over a public, authenticated channel. All information transmitted through this channel is considered publicly accessible and treated as part of the protocol’s output. By appropriately labeling each classical message, information-theoretic techniques can be employed to ensure authentication of the classical communication channel.

In general, a QKD protocol consists of two main phases. Firstly, both parties share a maximally entangled state through a secure quantum channel. Next, they apply a key distillation scheme to extract the final secret key. Consequently, for the security analysis of QKD, it suffices to establish the security of the underlying key distillation process. A schematic overview of the complete key distillation scheme is provided in Table III.

Before proceeding with the security analysis, we must ensure that the key generation scheme is correct and device-independent. Specifically, if an adversary attempts to construct a correlated system and interact with the protocol in parallel with the legitimate parties, their probability of winning the game should remain negligibly small. Further, the generated raw key should be distinguishable, barring a small fraction attributable to noise tolerance.

Therefore, prior to initiating the final key security analysis using the smooth minimum-entropy framework proposed by Renner [61, 67], we demonstrate in Section IV A that our scheme is ϵ -correct. Section IV B establishes the device independence of our protocol, and Section IV C ensures the security of the raw key.

A. Correctness of Our Protocol

In this section, we show the correctness of our protocol using the definition of ϵ -correct.

Definition IV.1. (ϵ -correct) *A quantum key distribution protocol is ϵ -correct [65, 67] if given a security parameter $\epsilon \geq 0$, Alice and Bob agree on a k -bit key $K \in \{0, 1\}^k$, except with some failure probability at most ϵ i.e. both parties achieve the key streams K_A, K_B respectively, such that $\Pr(K_A \neq K_B) \leq \epsilon$.*

We now show the correctness of our proposed DIQKD protocol by establishing a suitable ϵ .

Theorem IV.2. *The proposed QKD scheme guarantees an ϵ -correctness level, which is defined as $\epsilon_{correct} = [1 - (1 - \eta)^k]$. Here, ‘ k ’ represents the length of the entire raw key, and ‘ η ’ is the tolerable noise parameter.*

Proof: See Appendix A. □

B. Fully Device Independency of Our Protocol

We now turn our attention to the security of the overall protocol, which can be analyzed in two parts: the security of the fully device-independent testing phase and the security of the quantum key distillation phase.

In generic models of FDIQKD protocols, Bell nonlocality serves as a fundamental principle for verifying device independence [18, 67]. The key idea involves the use of Bell inequalities [18, 78], which are constraints that must be satisfied by any theories based on local hidden variables. A violation of these inequalities indicates the presence of correlations that cannot be explained by classical means, thereby revealing inherently quantum and nonlocal behavior. Importantly, such violations can be observed solely through input-output statistics, without any assumptions about the internal workings of the devices involved. This feature allows Bell inequality violations to serve as a powerful tool for establishing device independence, guaranteeing that the security or performance of a protocol is independent of the specific physical implementation.

Our protocol is based on the impossible colouring game, a pseudo-telepathy game constructed using the Kochen-Specker theorem. This theorem explores the impossibility of assigning deterministic outcomes, interpreted as a $\{0, 1\}$ colouring, to a certain set of vectors in \mathbb{R}^d , under the following two constraints: (i) only one vector in any orthogonal pair may be assigned the value 1, and (ii) at least one vector in every orthogonal triplet must be assigned the value 1. Such

sets are known as Kochen-Specker sets. The impossibility of such a colouring illustrates a fundamental feature of quantum mechanics known as contextuality [79].

Contextuality refers to the phenomenon in which the outcome of measuring an observable depends not solely on the system, but also on the specific set of compatible measurements performed alongside it, referred to as the context. This feature is fundamental to the impossible colouring game. In this game, two players receive orthogonal contexts drawn from a Kochen-Specker set and must assign values of 0 or 1 to each vector. They are promised that one vector in their input is identical to a vector in the other player’s input, although they do not know which one. Their task is to assign the value 1 to this shared vector. There is a nonzero probability that both players will select the same vector. However, any classical deterministic strategy must assign definite $\{0, 1\}$ values to the vectors, thereby violating the Kochen-Specker constraints and contradicting non-contextuality.

In contrast, a quantum strategy allows the players to always succeed. Their responses abide by the Kochen-Specker constraints and yield the shared vector, despite the impossibility of doing so in any classical non-contextual hidden variable model. This ability to maintain global consistency through local, context-dependent outcomes is not a technical artifact. It provides a concrete manifestation of contextuality as a physical principle. The fundamental challenge with contextuality, despite its close connection to nonclassical behavior, lies in the absence of a well-defined Bell inequality. Although it was commonly believed that contextuality implies Bell nonlocality, there existed no formal mathematical limit or inequality capable of capturing this implication. In particular, there was no Bell-type inequality whose violation could demonstrate that contextual behavior leads to nonlocal correlations.

Several works have attempted to bridge this conceptual gap. For instance, Kunkri et al. [80], Renner et al. [81], and Zimba et al. [82] explored the relationship by simulating Kochen-Specker-type contextual scenarios using nonlocal boxes or alternative geometric constructions. These approaches established structural analogies between contextuality and nonlocality but did not produce a concrete, experimentally testable inequality.

This gap was addressed in a series of papers by Cabello et al. [83–85], who showed that any Kochen-Specker contextuality scenario can be mapped to a bipartite nonlocality scenario. Significantly, the authors provided a constructive method for this transformation, including a procedure to derive a Bell inequality from the original contextual setup. This framework allows contextuality-based games, such

as the impossible colouring game, to be treated within the standard Bell framework, enabling formal, device-independent proofs based on violations of well-defined nonlocal constraints.

The algorithm as stated by Cabello et al. [84] used to perform this mapping is detailed, as follows.

1. First, check whether the Kochen–Specker set $S = \{|v_1\rangle, |v_2\rangle, \dots, |v_n\rangle\}$ is a state-independent contextuality (SI-C) set. To do this, construct the orthogonality graph G , where each vector in S corresponds to a node, and an edge is drawn between two nodes if the associated vectors are orthogonal. Then, verify whether both the chromatic number $\chi(G)$ and the fractional chromatic number $\chi_f(G)$ are strictly greater than the dimension d of the vectors. This condition is necessary for the set to exhibit state-independent contextuality.

(a) If the check fails, it implies the set is state-dependent contextual (SD-C). If it is an SD-C set, it can be converted to a SI-C set as stated in this article [84].

(b) If the check is true, this still does not confirm the set is SI-C. To confirm this, there must exist non-negative numbers w'_1, w'_2, \dots, w'_n and a number y' such that $0 \leq y' < 1$, satisfying the following conditions: for all independent sets \mathcal{I} in the graph G , we have $\sum_{i \in \mathcal{I}} w_i \leq y$, and

$$\left(\sum_i w_i \Pi_i \right) - \mathbb{I} \text{ is positive semi-definite}$$

where \mathbb{I} is the $d \times d$ Identity operator. If these conditions hold, the set is indeed SI-C. Otherwise, repeat the process described earlier to obtain an SI-C set. Maximize $\sum_i w'_i$ to obtain a unique set of weights $\{w_i\}_{i=1}^n$ and the corresponding number y .

Once these steps are done, we obtain a new graph \mathcal{G} generated from G and a new set S' derived from S . In our case, based on the Conway–Kochen vector set [70], we obtain an orthogonality graph \mathcal{G} as shown in Figure 2. We find that $\chi(\mathcal{G}) = 4$ and the fractional chromatic number $\chi_f(\mathcal{G}) = 3.2$, confirming that the set is not state-dependent contextual (SD-C). To verify that it is state-independent contextual (SI-C), we check for the existence of a tuple (w_1, \dots, w_{31}, y) satisfying the conditions of step (1b). Once a feasible tuple is found, we maximize $\sum w_i$ to obtain a unique solution.

Our implementation uses Python, specifically the libraries `numpy`, `networkx`, and `cvxpy`, ex-

ecuted in a Google Colab environment with a 2.4 GHz CPU and 24 GB RAM. Since the verification involves both semidefinite and linear programming, we use the `Splitting Cone Solver (SCS)` package. The solver returns a valid solution $(w_i)_{i=1}^{31}$ with $y = 0.999993642346489$.

2. Set the rank-one projections as $\Pi_i := |v_i\rangle\langle v_i|$. From the previous step, besides obtaining \mathcal{G} and S' , we also obtain another set $\{w_1, w_2, \dots, w_n, y\}$. We assign the weights associated with each Π_i and its corresponding node in \mathcal{G} as $W_i := \frac{w_i}{y}$. Note that $\sum_i W_i > d$.

We define $\alpha(\mathcal{G}, W)$ to be the weighted independence number of the graph \mathcal{G} , where the i -th node is assigned the weight W_i , and $W := \{W_i\}_{i=1}^n$.

Now, denoting $\vartheta(G, W)$ as the weighted Lovász number [86], we get the following contextuality inequality:

$$\sum_{i \in V(\mathcal{G})} W_i P(\Pi_i = 1) - \sum_{(i,j) \in E(\mathcal{G})} \max(W_i, W_j) P(\Pi_i = 1, \Pi_j = 1) \stackrel{NCHV}{\leq} \alpha(\mathcal{G}, \{W_i\}_{i=1}^n) \stackrel{QT}{\leq} \vartheta(G, \{W_i\}_{i=1}^n).$$

Note that “NCHV” in this inequality stands for Non-Contextual Hidden Variable Theories. We calculate normalized weights $W_i := \frac{w_i}{0.999993642346489}$. The 31 rays v_i from the Conway–Kochen set, alongside their corresponding normalized weights W_i is mentioned in Table II. We compute the weighted independence number $\alpha(\mathcal{G}, \{W_i\}_{i=1}^{31})$. It is of note that the independent set $\mathcal{I}' = \{2, 4, 6, 11, 12, 14, 17, 20, 30\}$ yields the maximum total weight. Therefore, the weighted independence number is given by $\alpha(\mathcal{G}, \{W_i\}) = \sum_{i \in \mathcal{I}'} W_i = 1.0000112242568169$. We skip the calculation for the weighted Lovász number, as it is computationally cumbersome, and it is enough to focus on the classical bound for the verification process.

3. We prepare our entangled two-state qudit system $|\psi\rangle := \sum_{k=0}^{d-1} |k\rangle |k\rangle$ and set Alice’s and Bob’s vector set as S' and \bar{S}' , where \bar{S}' is the complex conjugate of the elements of S' . Now we have

the following Bell-inequality:

$$\sum_{i \in V(\mathcal{G})} w_i P(\Pi_i^A = 1, \Pi_i^B = 1) - \left(\sum_{(i,j) \in E(\mathcal{G})} \frac{\max(W_i, W_j)}{2} \right) \left[P(\Pi_i^A = 1, \Pi_j^B = 1) + P(\Pi_j^A = 1, \Pi_i^B = 1) \right] \stackrel{LHV}{\leq} \alpha(\mathcal{G}, \{W_i\}_{i=1}^n).$$

Note that $P(\Pi_i^A = 1, \Pi_j^B = 1)$ is the probability that Alice obtains outcome 1 for measurement Π_i on her particle and Bob obtains outcome 1 for measurement Π_j on his particle, and that ‘‘LHV’’ stands for Local Hidden Variable Theories.

Hence, from the discussions so far, we get the following inequality.

$$\sum_{i \in V(\mathcal{G})} w_i P(\Pi_i^A = 1, \Pi_i^B = 1) - \left(\sum_{(i,j) \in E(\mathcal{G})} \frac{\max(w_i, w_j)}{2} \right) \cdot [P(\Pi_i^A = 1, \Pi_j^B = 1) + P(\Pi_j^A = 1, \Pi_i^B = 1)] \stackrel{LHV}{\leq} 1.0000112242568169.$$

Here, the calculations have been carried out with respect to the orthogonality graph of the Conway-Kochen Set of 31 vectors, which is depicted in Figure 2.

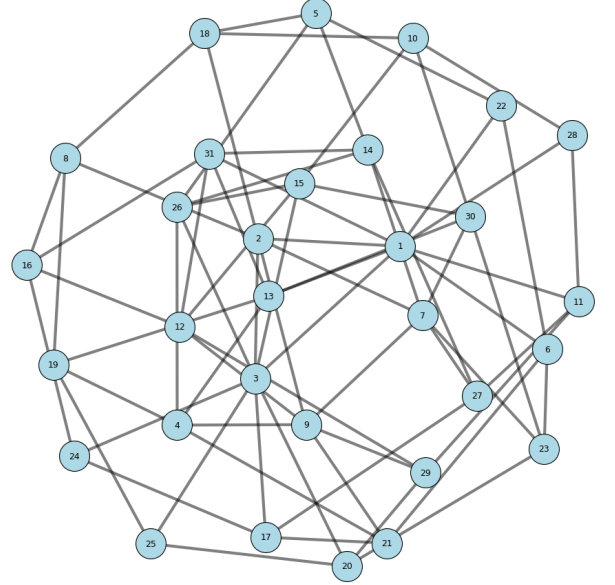


Figure 2: The orthogonality graph of the Conway-Kochen Set of 31 vectors, denoted as \mathcal{G} . Note that an edge exists between two nodes if and only if the vectors corresponding to the nodes are orthogonal to each other. Extensive details about the vectors are provided in Table II.

Further, in order to ensure device independence in the Impossible Colouring game, it is necessary to understand the observed success probability, particularly to distinguish classical strategies from quantum ones. Since classical strategies are bounded by a dimension-dependent success threshold, any observed violation of this bound certifies nonclassical behavior purely from statistics, without relying on assumptions about the devices.

Theorem IV.3. *Let a d -dimensional Impossible Colouring game be played between two parties. Then the maximum success probability achievable by any classical strategy is $\frac{1}{d}$.* (5)

Proof. See Appendix B. \square

For our protocol, we now state the specific instance of Theorem IV.3 for the case $d = 3$.

Corollary IV.4. *When a 3-dimensional Impossible Colouring game is played among 2 parties, then the best possible approach of winning this game for these 2 parties will have a probability of $\frac{1}{3}$.*

It can be seen that for the quantum case, from the

Node i	Rays v_i	Corresponding weights W_i
1	$(1, 0, 0)^T$	0.25799809370143945
2	$(0, 0, 1)^T$	0.19999263759649782
3	$(0, 1, 0)^T$	0.2579980937016148
4	$(-1, 1, -1)^T$	0.12473071346150894
5	$(-1, 2, -1)^T$	0.04198675640899053
6	$(0, 2, -1)^T$	0.07527393320356464
7	$(-1, 1, 0)^T$	0.19999975889766655
8	$(-1, 2, 0)^T$	0.04198868808244714
9	$(1, 1, 0)^T$	0.1999997588976661
10	$(-1, 2, 1)^T$	0.0419867564089987
11	$(0, 2, 1)^T$	0.0752739332035787
12	$(-1, 1, 1)^T$	0.12473071346150441
13	$(0, 1, 1)^T$	0.14075323938552295
14	$(1, 1, 1)^T$	0.12473071346150931
15	$(1, 0, 1)^T$	0.1407532393865908
16	$(2, 1, 1)^T$	0.04198675640808494
17	$(2, 0, 1)^T$	0.07527393320356927
18	$(2, 1, 0)^T$	0.041988688083343585
19	$(2, 1, -1)^T$	0.04198675640808829
20	$(2, 0, -1)^T$	0.07527393320357453
21	$(-1, 1, 2)^T$	0.07527928769251237
22	$(0, 1, 2)^T$	0.04198226094368069
23	$(1, 1, 2)^T$	0.07527928769251353
24	$(-1, 0, 2)^T$	0.0419822609427853
25	$(1, 0, 2)^T$	0.041982260942795356
26	$(-1, 0, 1)^T$	0.1407532393865908
27	$(-1, -1, 2)^T$	0.07527928769251417
28	$(0, -1, 2)^T$	0.04198226094369912
29	$(1, -1, 2)^T$	0.07527928769251518
30	$(-1, -1, 1)^T$	0.12473071346150935
31	$(0, -1, 1)^T$	0.14075323938552078

Table II: The table of nodes and their corresponding rays and weights of graph \mathcal{G} as depicted in Figure 2

proof of Corollary IV.4 (A), that the probability

$$P(\Pi_i^A = 1, \Pi_j^B = 1) = \begin{cases} \frac{1}{3}, & \text{if } i = j \\ 0, & \text{otherwise} \end{cases}$$

Thus, the left-hand side of the inequality simplifies to $\frac{1}{3} \sum_i W_i = 1.066663494447466$, which is clearly greater than the right-hand side of the inequality mentioned in Equation 5. Therefore, the quantum case violates this inequality, thereby establishing the device independence of the proposed protocol.

In a generic classical noncontextual or local hidden-variable model with their associated weighted graph

[86], each event is assigned a predetermined value: either it occurs, which is counted as 1, or it does not (to be counted as 0). Since mutually exclusive events cannot both occur, such models correspond to choosing independent sets in the exclusivity graph G . The maximum total weight attainable in any classical strategy is therefore upper bounded by the *weighted independence number* $\alpha(G, w)$.

Further, as shown in some works in the literature such as [65], if Alice and Bob each receive three particles from an \mathcal{N} -partite quantum state, with the remaining $\mathcal{N} - 3$ held by an adversary (Eve), the protocol can still exhibit device independence provided the observed success probability p in the Impossible Colouring game lies in $[1 - \eta, 1]$. Since this game is a pseudo-telepathy game, such performance cannot be achieved by classical or adversarially correlated strategies. As we will later see, the threshold η is 18.11%, and the result in Corollary IV.4 implies that any substantial correlation with Eve would be detectable during the testing phase. This provides an alternative perspective, validating the conclusion that our protocol achieves device-independent quantum key distribution.

C. Security of Raw Key

In this section, we focus on the key aspect of the security analysis, namely the security of the key distillation phase. In a quantum key distillation protocol, Alice and Bob receive inputs from \mathcal{N} -dimensional Hilbert spaces $\mathcal{H}_A^{\otimes \mathcal{N}}$ and $\mathcal{H}_B^{\otimes \mathcal{N}}$, respectively, and proceed through the following subprotocols:

- i. Random permutation of the subsystems,
- ii. Parameter estimation,
- iii. Block-wise measurement, and
- iv. Classical post-processing.

A schematic representation of the key distillation procedure, detailing each of the above subprotocols, is provided in Table III.

In classical cryptographic protocols, security is usually defined in terms of random systems by measuring their distance from an ideal system, which is secure by definition [65]. The ideal system for a classical Key Distribution scheme generates a uniform random key at one end, with all interfaces being completely independent of one another. Since the adversary must guess uniformly from the set of all possible keys, the key is considered secure by construction, since each possible string occurs with equal probability. A key is therefore regarded as secure if no

significant distinction can be made between the real and ideal systems that generate it.

In the quantum setting, however, the adversary (Eve) may prepare a correlated quantum system to gain information about the measurements and corresponding raw key bits shared between the parties. If Eve's system is uncorrelated with the shared quantum state of the parties, then she cannot obtain any information. In this scenario, the overall system is considered secure if Eve's subsystem is uncorrelated with that of Alice and Bob, and the joint state appears to be maximally mixed from Eve's perspective. According to the key distillation phase, the key bits generated after the block-wise measurement phase are referred to as the raw key.

In general, the closeness measure is defined using the definition of statistical distance as

Definition IV.5. (*Statistical Distance:*) [65] Let X_0 and X_1 be two random variables over a finite set \mathcal{C} . Then the statistical distance $\Delta(X_0, X_1)$ is defined as:

$$\Delta(X_0, X_1) = \frac{1}{2} \sum_{x \in \mathcal{C}} |\Pr(X_0 = x) - \Pr(X_1 = x)|.$$

This notion of quantifying closeness in the classical setting using statistical distance leads to the following theorem, which illustrates the security of the generated raw key. Further, we shall also provide the formal definition of distinguishability in the context of this paper. We note that the statistical distance draws parallel with Total Variation Distance (TVD) of probability measures [87].

Definition IV.6. *The raw key bit generated in any protocol is said to be η -distinguishable if for any Probabilistic Polynomial Time (PPT) adversary, $|\Pr(\text{adversary guesses raw bit correctly}) - \Pr(\text{adversary guesses random bit correctly})| \leq \eta$*

Then we have the following theorem.

Theorem IV.7. *In the proposed protocol, each raw key bit that is generated is at most η -distinguishable from a randomly generated bit, where η represents the tolerable noise parameter for the protocol.*

Proof: See Appendix C. □

D. Security of Active (Final) Key

In this section, we shall provide the length of the active key and subsequently derive the key rate. The Lo-Chau security proof [88] was one of the first to rigorously establish the theoretical security of QKDs, specifically for the BB84 protocol [2], and was later extended to DIQKD protocols. It introduced the reduction of QKD to entanglement purification protocols. Following this, Shor and Preskill [89] simplified the Lo-Chau proof by connecting it to Calderbank-Shor-Steane (CSS) codes [90, 91]. These proofs were groundbreaking and laid the foundation for QKD security. Renner's proof [61] offers another comprehensive, realistic, and practically applicable security framework. It addresses a wider range of practical issues, provides finite-key security guarantees, and ensures composable security. In 2020, Tsurumaru [92] simplified the idea of QKD security by showing a mathematical equivalence between the security proofs following Mayers(?)–Shor–Preskill and that of Renner's using the Leftover Hashing Lemma. In this paper, we will follow Renner's approach in validating security and estimating the key rate of our given scheme. It is to be noted that our proposed scheme is inherently *one-way* [61] and does not require noisy preprocessing. Specifically, after the measurement of the entangled subsystems, Alice and Bob proceed directly to an information reconciliation protocol, wherein Bob computes an estimate of Alice's raw key using the information exchanged over an authenticated classical channel. This streamlined design avoids additional classical interaction and preprocessing steps, thereby reducing operational complexity. As a result, the protocol remains efficient and practical, particularly in low-latency or high-noise quantum network environments.

 Device Independent Quantum Key Distillation Scheme for QKD_{PE, BM, CPP}

Parameters:

PE: Parameter estimation

BM: Block wise Measurement

CPP: Classical Post-Processing

 \mathcal{N} : Number of input systems ($\mathcal{N} \geq p + qn$) (The symbols $p, q,$ and n follow from Table I)

Alice	Bob
Input system: $\mathcal{H}_A^{\otimes \mathcal{N}}$	Input system: $\mathcal{H}_B^{\otimes \mathcal{N}}$

Random permutation of subsystem	$\xleftrightarrow{\pi}$	Random permutation of subsystem
---------------------------------	-------------------------	---------------------------------

$\mathcal{H}_A^{\otimes p}$	$\xleftrightarrow{\text{PE}}$	$\mathcal{H}_B^{\otimes p} \rightarrow (\text{accept/abort})$
$(\mathcal{H}_A^{\otimes q})^{\otimes n}$	$\xleftrightarrow{\text{BM}^{\otimes n}}$	$(\mathcal{H}_B^{\otimes q})^{\otimes n}$
$(u_1, u_2, \dots, u_n) \rightarrow K_A^R$	$\xleftrightarrow{\text{CPP}}$	$(v_1, v_2, \dots, v_n) \rightarrow K_B^R$
output K_A^F		output K_B^F

Table III: Schematic overview of the proposed device-independent key distillation protocol.

We shall now determine the key rate r based on the work of Portman and Renner [61, 67]. We make use of the tolerable noise parameter η which is equivalent to quantum bit error rate in [61, 67]. In this paper, η represents the Quantum Trit Error Rate (QTER). In this context, we focus on the modular approach to security analysis proposed by Portman and Renner [67] in 2022. All security proofs share a common goal, which is to establish a relationship between the information available to authorized parties and the information that could have been obtained by Eve. In this regard, analysis of the key rate of the protocol is fundamental to its computation. The key rate of the quantum key distribution scheme is provided as follows.

$$\text{Key rate} = \min_{\sigma_{AB} \in \Gamma} H(X|E) - H(X|Y),$$

where the set Γ is defined as

$$\Gamma = \{\sigma_{AB} : P_W^{\sigma_{AB}} \in \mathcal{Q}\}.$$

Here, after applying a set of positive operator-valued measurements (POVMs) \mathcal{M} , the state σ_{AB} is mapped to a probability distribution $P_W^{\sigma_{AB}}$, that must lie in the set \mathcal{Q} which is defined as the collection

of statistics for which the protocol does not abort. In our protocol, we follow the same idea as [61] where the set Γ depends on the error rate η and is characterized by the following condition which is as follows: For all measurement bases of Alice and Bob as stated in Algorithm 1, and for all vectors of Alice and Bob with respect to their respective bases (denoted as v_A and v_B respectively) such that $v_B \neq v_\ell$ and

$$v_A \neq \begin{cases} v_1, & \text{if } v_1 = v_\ell, \\ v_2, & \text{otherwise.} \end{cases}$$

then the following inequality

$$(\langle v_B | \otimes \langle v_A |) \sigma_{AB} (|v_A\rangle \otimes |v_B\rangle) \leq \frac{\eta}{2}, \quad (6)$$

holds.

It is of note that the equality condition mentioned in [61], is relaxed in our context. The reasoning behind it is due to the fact that for the case when we have only the Bell-state that we require, the left hand side of Equation 6 drops to 0. Now, we present the following theorem.

Theorem IV.8. *Let \mathcal{H}_A and \mathcal{H}_B be three-dimensional Hilbert spaces, and let $\sigma_{ABE} \in P(\mathcal{H}_A \otimes$*

$\mathcal{H}_B \otimes \mathcal{H}_E$) be the shared density operator of Alice, Bob, and Eve. Suppose σ_{XYE} is the resulting state obtained from σ_{ABE} by performing orthonormal measurements on the spaces \mathcal{H}_A and \mathcal{H}_B . Then

$$\begin{aligned}
& H(X|E) - H(X|Y) \\
\geq & 1 + \lambda_0 \log_3 \lambda_0 + \lambda_1 \log_3 \lambda_1 + \lambda_2 \log_3 \lambda_2 \\
& + \lambda_3 \log_3 \lambda_3 + \lambda_4 \log_3 \lambda_4 + \lambda_5 \log_3 \lambda_5 \\
& + \lambda_6 \log_3 \lambda_6 + \lambda_7 \log_3 \lambda_7 + \lambda_8 \log_3 \lambda_8 \\
& - (\lambda_0 + \lambda_1 + \lambda_2) \log_3 (\lambda_0 + \lambda_1 + \lambda_2) \\
& + (\lambda_0^2 + \lambda_1^2 + \lambda_2^2) \log_3 (\lambda_0^2 + \lambda_1^2 + \lambda_2^2) \\
& - (\lambda_3 + \lambda_4 + \lambda_5) \log_3 (\lambda_3 + \lambda_4 + \lambda_5) \\
& + (\lambda_3^2 + \lambda_4^2 + \lambda_5^2) \log_3 (\lambda_3^2 + \lambda_4^2 + \lambda_5^2) \\
& - (\lambda_6 + \lambda_7 + \lambda_8) \log_3 (\lambda_6 + \lambda_7 + \lambda_8) \\
& - (\lambda_6^2 + \lambda_7^2 + \lambda_8^2) \log_3 (\lambda_6^2 + \lambda_7^2 + \lambda_8^2)
\end{aligned}$$

where λ_i 's are eigenvalues of σ_{AB} i.e. the density operator of the joint system of Alice and Bob with respect to the 3-dimensional Bell basis mentioned in Section III C.

Proof: See Appendix D. \square

It is important to note that the above theorem characterizes the key rate as the minimum of the specified entropy difference. The proof of Theorem IV.8 is primarily non-constructive, meaning that it establishes the result in principle through existence arguments, rather than by explicitly constructing the solution.

We identify the exact diagonal matrix in Γ that satisfies the required constraints, by adopting an approximation. This approximation matrix construction arises from the assumption that all of the Bell-states except the first one (which is used in our measurements) is equally probable. This approximate form is computationally tractable where we choose the diagonal matrix as

$$\text{diag} \left(1 - c\eta, \underbrace{\frac{c\eta}{8}, \dots, \frac{c\eta}{8}}_{8 \text{ times}} \right),$$

where c is a tunable parameter. This choice of diagonal matrix comes from Theorem IV.8. This simplification allows for meaningful analytical progress while preserving the essential structure required for the analysis. We find the general qutrit mutual information, which is

$$\begin{aligned}
H(X : Y) &= H(X) + H(Y) - H(X, Y) \\
&= H(\sigma_X) + H(\sigma_Y) - H(\sigma_{XY}) \\
&= 2 + (\log_3 (\lambda_0^2 + \lambda_1^2 + \lambda_2^2) - 1) (\lambda_0^2 + \lambda_1^2 + \lambda_2^2) \\
&\quad + (\log_3 (\lambda_3^2 + \lambda_4^2 + \lambda_5^2) - 1) (\lambda_3^2 + \lambda_4^2 + \lambda_5^2) \\
&\quad + (\log_3 (\lambda_6^2 + \lambda_7^2 + \lambda_8^2) - 1) (\lambda_6^2 + \lambda_7^2 + \lambda_8^2)
\end{aligned}$$

Particularly for our case, the mutual information is:

$$\begin{aligned}
H(X : Y) &= \frac{1}{32} \left(3c^2\eta^2 \log_3 \left(\frac{c^2\eta^2}{64} \right) \right. \\
&\quad - 8(c^2\eta^2 + 8(c\eta - 1)^2) \log_3 \left(\frac{c^2\eta^2}{24} + \frac{(c\eta - 1)^2}{3} \right) \\
&\quad \left. + (c^2\eta^2 + 32(c\eta - 1)^2) \log_3 \left(\frac{c^2\eta^2}{96} + \frac{(c\eta - 1)^2}{3} \right) \right)
\end{aligned}$$

We then followed up by analyzing the graph of the mutual information as a function of the error rate, ranging from 0 to 33.33%, and discretized the parameter c from -2.0 to 2.5 in steps of 0.5 , excluding $c = 0$. We immediately observe that the mutual information values for $c < 0$ can exceed 1, which violates the fundamental bound $H(X : Y) \leq \log_3 3 = 1$ for qutrit systems. In fact, in Figure 3, we plot the mutual information as a function of the error rate (i.e., noise tolerance), using several discretized values of the parameter c .

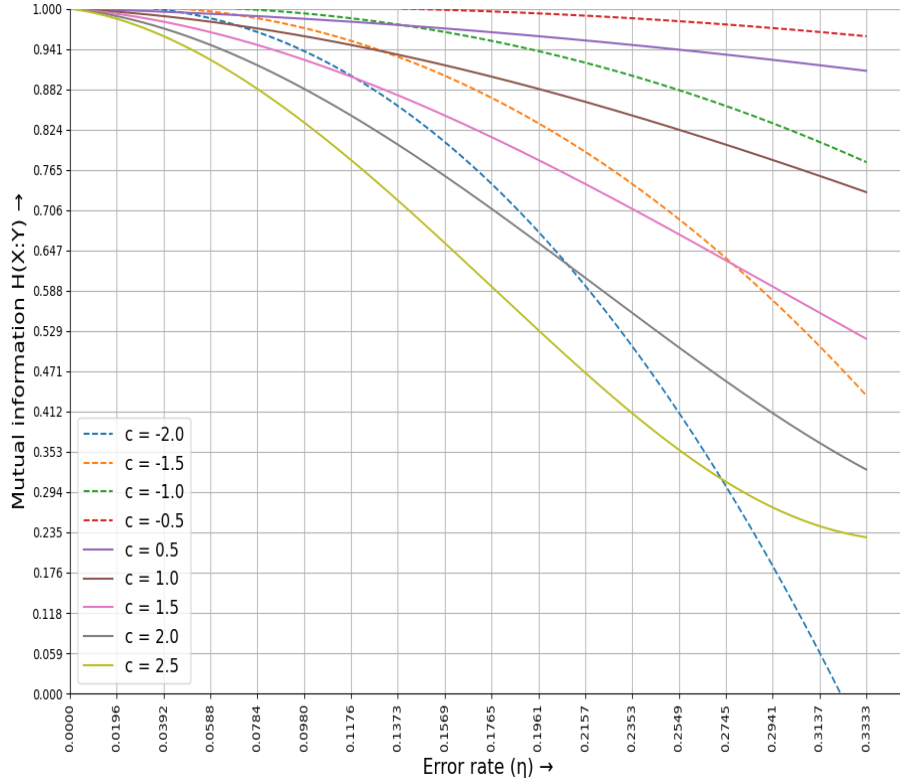


Figure 3: Variation of mutual information $H(X : Y)$ with error rate η for different values of the correlation parameter c . Mutual information decreases as the error rate increases, with the rate of decline dependent on c . Negative values of c (dashed lines) show mutual information greater than 1, which is contradictory, and are thus discarded, while positive values (solid lines) retain high mutual information at most 1. The curves correspond to: **dashed blue** for $c = -2.0$, **dashed orange** for $c = -1.5$, **dashed green** for $c = -1.0$, **dashed red** for $c = -0.5$, **solid violet** for $c = 0.5$, **solid brown** for $c = 1.0$, **solid magenta** for $c = 1.5$, **solid gray** for $c = 2.0$, and **solid olive** for $c = 2.5$

We note that the left-hand side of the inequality simplifies to $\max\left(0, \frac{1}{3} - \frac{c\eta}{4}\right)$, and thus to satisfy the inequality, we note that $c \geq 2$ should suffice for $0 \leq \eta \leq \frac{1}{3}$.

We choose $c = 2$ to maximize the inequality and proceed with the calculations. Thus, assuming the entangled system is trusted by Alice and Bob to a point where they skip the testing phase of Algorithm 1, the key rate is:

$$r \gtrsim 2\eta \log\left(\frac{\eta}{4}\right) - \frac{3\eta \log\left(\frac{3\eta}{4}\right)}{2} - (2\eta - 1) \log(1 - 2\eta) + \frac{(3\eta - 2) \log\left(1 - \frac{3\eta}{2}\right)}{2} + \frac{(\eta^2 + 8(2\eta - 1)^2) \log\left(\frac{33\eta^2}{8} - 4\eta + 1\right)}{8} + 1 \quad (7)$$

This directly follows from Theorem IV.8.

We plot the graph in Figure 4 for Equation 7 and find that rate = 0 when $\eta \approx 18.10610749073431\%$ and beyond.

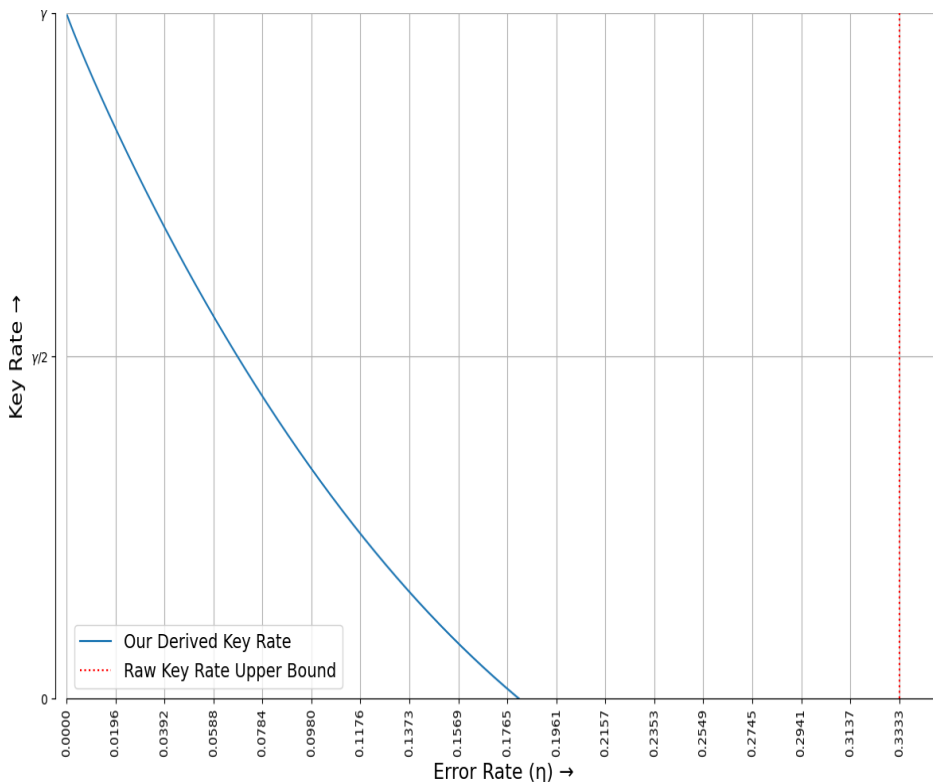


Figure 4: Key rate as a function of error rate η . The solid blue curve represents our derived key rate, which decreases monotonically with increasing error. The vertical red dashed line indicates the raw key rate upper bound, beyond which secure key generation is not feasible. The plot highlights the trade-off between noise and secure communication rate in the protocol.

This represents a significant advantage, as it implies that the key rate remains constant regardless of the choice of n (Table I). In the ideal scenario where $\eta = 0$, the key rate evaluates to $r = 1$, indicating a 100% key rate under zero noise.

However, since parameter estimation needs to take place between Alice and Bob, so that they can verify if they receive the state $\frac{|00\rangle + |11\rangle + |22\rangle}{\sqrt{3}}$, a fraction of their outputs with their respective inputs will have to be made public, and thus these cannot influence the key rate. In particular, if γ of the total outputs are used to verify the Bell state provided (as stated in the testing phase of Algorithm 1), the new key rate should be $r' := \max\left\{0, \frac{\gamma}{2} \cdot \inf \sum r(\tilde{\sigma}_{XY})\right\}$, where the infimum is calculated over all possible values of $\tilde{\sigma}_{XY}$ such that the corresponding input state σ_{AB} satisfies the Bell inequality as stated in IV B. The factor $\frac{1}{2}$ is chosen as Bob has two possible inputs, depending on which of the two vectors of Alice he chooses in each of the iterations, whereas Alice's input is fixed.

However, we can approximate it, as both the bases chosen by Bob are independent of each other, and thus we get $r' \gtrsim \max\left\{0, \frac{\gamma}{2} \cdot 2 \cdot r\right\} = \max\{0, \gamma \cdot r\}$.

Table IV provides a comparison between our protocol and several standard DIQKD protocols, emphasizing key differences such as device assumptions, noise tolerance, the key rate in the zero-noise regime, the dependence on the parameter n , and whether a finite-key analysis is included.

It is also of note that existing DIQKD protocols, thus far, exhibit significantly lower key rates. The highest known key rate is achieved by the BB84 protocol and its variants, where the key rate is given by $R_{\text{BB84}} = 1 - 2h(\eta)$ [67], which is also independent of the parameter n . However, as illustrated in Figure 4, which plots the key rate r against the noise parameter η (error rate), our protocol surpasses the key rate of BB84 (including its variants such as Asymmetric BB84 and BBM92 [93]). Notably, our key rate remains positive until a noise threshold of 18.11%, beyond which it drops to zero. This feature is par-

ticularly significant for the practical deployment of DIQKD protocols in noisy or near-term intermediate-scale quantum (NISQ) environments. The ability to sustain a comparatively higher key rate in the pres-

ence of noise renders our protocol well-suited for implementation on current quantum hardware, where noise is a fundamental limitation.

	Reichardt et al. [94]	Vazirani et al. [16]	Tomamichel et al. [11]	Tomamichel et al. [9]	Zhen et al. [14]	Proposed Protocol
Nature of Protocol	E91 based [12]	Game based [24]	Asymmetric BB84 based [2]	BBM92 based [93]	Game Based [66]	Game Based [95]
Device Assumptions	None	None	Trusted Alice*	Trusted Alice*	None	None
Noise Tolerance	0%	1.2%	11%	1.5%	3.1%	18.11% (Highlighted in Figure 4)
Key rate (Zero Noise)	0.5%	2.5%	100%	22.8%	100%**	100%**
Finite key Analysis	No	No	Yes	Yes	Yes	Yes
Dependency on n in key rate	No	Yes	No	No	Yes	No

Table IV: Security Comparison of DIQKD protocols

* Using results of self-testing [96, 97], one can reduce the assumption to memoryless for Alice.

** The key rate of this protocol depends on the term γ where $0 < \gamma \leq 1$. The key rate of 100% is achieved when $\gamma = 1$ i.e. the ideal scenario where nothing is discarded in parameter estimation and the noise tolerance is zero.

V. CONCLUSION

In this paper, we propose a simple ternary device independent quantum key distribution protocol based on the two-party Impossible Colouring pseudo-telepathy game. The simplicity of the protocol arises from the fact that it does not require multiple measurement bases. On the contrary, a single test is sufficient to guarantee correctness, device independence, and raw key security. Moreover, the game is impossible to win classically, which ensures that no classical attack is possible. We demonstrate that the final key security directly follows from the concept of smooth minimum-entropy, which quantifies the randomness in a system and serves as the standard theoretical definition of security in quantum cryptography.

Our protocol employs a qutrit circuit to create 3-dimensional Bell states, which is advantageous because it requires fewer resources, lower circuit depth,

and offers a higher information-carrying capacity compared to traditional qubit-based circuits. This enhances both the efficiency and scalability of the protocol. Furthermore, the use of qutrits contributes to improving the key rate and the robustness of the protocol.

We also show that our proposed protocol exhibits a key rate advantage over established protocols such as BB84 [2], VVQKD [17], and other pseudo-telepathy-based QKD protocols [14, 65]. Notably, the key rate is independent of the number of subsystems involved in blockwise measurements, offering scalability benefits. In the future, one could extend this approach to more than two users, leading to a Quantum Conference Key Agreement (QCKA) [98]. Further, the exploration of non-local games, such as the quantum XOR game or non-zero-sum games, could provide alternative foundations for constructing DIQKD protocols that have not yet been thoroughly investigated.

We comment that extensive cryptanalytic studies on this protocol would be a valuable direction for future research.

Another important future avenue involves refining the representation of the special set of matching entangled qutrits between two parties, often referred to as the Γ set [61], which could help optimize our key rate formula and extend the maximum tolerable error bound. Our protocol is inherently one-way and does not rely on noisy preprocessing. However, incorporating advantage distillation and preprocessing could enhance the error threshold beyond the current limit of 18.11%. Furthermore, in the future, one may use the Impossible Colouring game and can extend the QKD protocol for more than two users, which is known as Quantum Conference Key Agreement (QCKA) [98].

We also mention that if qubits were to be used in the Impossible Colouring game in higher dimensions (i.e., $d = 2^m$ for $m > 1$), one would need to maintain a raw key error rate below 2^{-m} . This raw key error rate is lower compared to our approach, where we use $d = 3$ and tolerate an error rate up to $\frac{1}{3}$ (33.33%), ensuring a more robust security model.

In conclusion, the proposed device-independent quantum key distribution protocol based on the Impossible Colouring pseudo-telepathy game presents a significant advancement in quantum cryptography. Overall, this work lays the groundwork for future developments in secure quantum communication using non-local pseudo-telepathy games.

DATA AVAILABILITY

All data and code supporting the findings of this manuscript are available from the authors upon reasonable request.

ACKNOWLEDGMENTS

R.S.S. acknowledges funding through MSCA (Grant No. 101126667/ Ramon Llull AIRA). Prof. Avishek Adhikari receives partial support from the DST-FIST Project, funded by the Government of India, under Sanction Order SR/FST/MS-I/2019/41.

-
- [1] Antonio Acin, Nicolas Gisin, and Lluís Masanes. From bell's theorem to secure quantum key distribution. *Physical review letters*, 97(12):120405, 2006.
- [2] Charles H Bennett and Gilles Brassard. Quantum cryptography: Public key distribution and coin tossing. *Theoretical computer science*, 560:7–11, 2014.
- [3] Yonggi Jo, Kwangil Bae, and Wonmin Son. Enhanced bell state measurement for efficient measurement-device-independent quantum key distribution using 3-dimensional quantum states. *Scientific reports*, 9(1):687, 2019.
- [4] Lov K Grover. A fast quantum mechanical algorithm for database search. In *Proceedings of the twenty-eighth annual ACM symposium on Theory of computing*, pages 212–219, 1996.
- [5] M.A. Nielsen and I.L. Chuang. *Quantum Computation and Quantum Information: 10th Anniversary Edition*. Cambridge University Press, 2010.
- [6] William K Wootters and Wojciech H Zurek. The no-cloning theorem. *Physics Today*, 62(2):76–77, 2009.
- [7] Antonio Acin, Serge Massar, and Stefano Pironio. Efficient quantum key distribution secure against no-signalling eavesdroppers. *New Journal of Physics*, 8(8):126, 2006.
- [8] Charles H Bennett. Quantum cryptography using any two nonorthogonal states. *Physical review letters*, 68(21):3121, 1992.
- [9] Marco Tomamichel, Serge Fehr, Jkdrzej Kaniewski, and Stephanie Wehner. A monogamy-of-entanglement game with applications to device-independent quantum cryptography. *New Journal of Physics*, 15(10):103002, 2013.
- [10] Marco Tomamichel, Serge Fehr, Jkdrzej Kaniewski, and Stephanie Wehner. One-sided device-independent qkd and position-based cryptography from monogamy games. In *Advances in Cryptology—EUROCRYPT 2013: 32nd Annual International Conference on the Theory and Applications of Cryptographic Techniques, Athens, Greece, May 26-30, 2013. Proceedings 32*, pages 609–625. Springer, 2013.
- [11] Marco Tomamichel, Charles Ci Wen Lim, Nicolas Gisin, and Renato Renner. Tight finite-key analysis for quantum cryptography. *Nature communications*, 3(1):634, 2012.
- [12] Artur K Ekert. Quantum cryptography based on bell's theorem. *Physical review letters*, 67(6):661, 1991.
- [13] Carl A Miller and Yaoyun Shi. Robust protocols for securely expanding randomness and distributing keys using untrusted quantum devices. *Journal of the ACM (JACM)*, 63(4):1–63, 2016.
- [14] Yi-Zheng Zhen, Yingqiu Mao, Yu-Zhe Zhang, Feihu Xu, and Barry C Sanders. Device-independent quantum key distribution based on the mermin-peres magic square game. *Physical Review Letters*, 131(8):080801, 2023.
- [15] Christiana Panayi, Mohsen Razavi, Xiongfeng Ma, and Norbert Lütkenhaus. Memory-assisted measurement-device-independent quantum key distribution. *New Journal of Physics*, 16(4):043005, 2014.

- [16] Umesh Vazirani and Thomas Vidick. Fully device independent quantum key distribution. *Communications of the ACM*, 62(4):133–133, 2019.
- [17] Umesh Vazirani and Thomas Vidick. Fully device independent quantum key distribution. *Physical review letters*, 113, 2014.
- [18] Nicolas Brunner, Daniel Cavalcanti, Stefano Pironio, Valerio Scarani, and Stephanie Wehner. Bell non-locality. *Reviews of modern physics*, 86(2):419–478, 2014.
- [19] Yonggi Jo and Wonmin Son. Key-rate enhancement using qutrit states for quantum key distribution with askew aligned sources. *Physical Review A*, 94(5):052316, 2016.
- [20] Ignatius W Primaatmaja, Koon Tong Goh, Ernest Y-Z Tan, John T-F Khoo, Shouvik Ghorai, and Charles C-W Lim. Security of device-independent quantum key distribution protocols: a review. *Quantum*, 7:932, 2023.
- [21] Wei Zhang, Tim van Leent, Kai Redeker, Robert Garthoff, René Schwonnek, Florian Fertig, Sebastian Eppelt, Wenjamin Rosenfeld, Valerio Scarani, Charles C-W Lim, et al. A device-independent quantum key distribution system for distant users. *Nature*, 607(7920):687–691, 2022.
- [22] Victor Zapatero, Tim van Leent, Rotem Arnon-Friedman, Wen-Zhao Liu, Qiang Zhang, Harald Weinfurter, and Marcos Curty. Advances in device-independent quantum key distribution. *npj quantum information*, 9(1):10, 2023.
- [23] Gilles Brassard, Anne Broadbent, and Alain Tapp. Quantum pseudo-telepathy. *Foundations of Physics*, 35:1877–1907, 2005.
- [24] John F Clauser, Michael A Horne, Abner Shimony, and Richard A Holt. Proposed experiment to test local hidden-variable theories. *Physical review letters*, 23(15):880, 1969.
- [25] Lana Sheridan and Valerio Scarani. Security proof for quantum key distribution using qudit systems. *Physical Review A—Atomic, Molecular, and Optical Physics*, 82(3):030301, 2010.
- [26] Quantum cryptography using larger alphabets. *Physical Review A*, 61(6):062308, 2000.
- [27] Nicolas J Cerf, Mohamed Bourennane, Anders Karlsson, and Nicolas Gisin. Security of quantum key distribution using d-level systems. *Physical review letters*, 88(12):127902, 2002.
- [28] G Molina-Terriza and J Řeháček. Triggered qutrits for quantum communication protocols. *Physical review letters*, 92(16):167903, 2004.
- [29] Bell-type test of energy-time entangled qutrits. *Physical review letters*, 93(1):010503, 2004.
- [30] Nurul T Islam, Charles Ci Wen Lim, Clinton Cahall, Bing Qi, Jungsang Kim, and Daniel J Gauthier. Scalable high-rate, high-dimensional time-bin encoding quantum key distribution. *Quantum Science and Technology*, 4(3):035008, 2019.
- [31] Yu I Bogdanov, MV Chekhova, SP Kulik, GA Maslennikov, AA Zhukov, CH Oh, and MK Tey. Qutrit state engineering with biphotons. *Physical review letters*, 93(23):230503, 2004.
- [32] Helle Bechmann-Pasquinucci and Asher Peres. Quantum cryptography with 3-state systems. *Physical Review Letters*, 85(15):3313, 2000.
- [33] Dagomir Kaszlikowski, Matthias Christandl, Kelken Chang, Artur Ekert, and CH Oh. Quantum cryptography based on qutrit bell inequalities. *Physical Review A*, 67(1):012310, 2003.
- [34] Thomas Durt, Nicolas J. Cerf, Nicolas Gisin, and Marek Żukowski. Security of quantum key distribution with entangled qutrits. *Phys. Rev. A*, 67:012311, Jan 2003.
- [35] Zhiguang Yan, Yu-Ran Zhang, Ming Gong, Yulin Wu, Yarui Zheng, Shaowei Li, Can Wang, Futian Liang, Jin Lin, Yu Xu, et al. Strongly correlated quantum walks with a 12-qubit superconducting processor. *Science*, 364(6442):753–756, 2019.
- [36] C Huerta Alderete, Shivani Singh, Nhung H Nguyen, Daiwei Zhu, Radhakrishnan Balu, Christopher Monroe, CM Chandrashekar, and Norbert M Linke. Quantum walks and dirac cellular automata on a programmable trapped-ion quantum computer. *Nature communications*, 11(1):3720, 2020.
- [37] Radhakrishnan Balu, Daniel Castillo, and George Siopsis. Physical realization of topological quantum walks on ibm-q and beyond. *Quantum Science and Technology*, 3(3):035001, 2018.
- [38] Frank Acasiete, Flavia P Agostini, J Khatibi Moqadam, and Renato Portugal. Implementation of quantum walks on ibm quantum computers. *Quantum Information Processing*, 19:1–20, 2020.
- [39] Shivani Singh, Cinthia H Alderete, Radhakrishnan Balu, Christopher Monroe, Norbert M Linke, and CM Chandrashekar. Universal one-dimensional discrete-time quantum walks and their implementation on near term quantum hardware. *Preprint at https://arxiv.org/abs/2001.11197*, 2020.
- [40] Jia-Qi Zhou, Ling Cai, Qi-Ping Su, and Chui-Ping Yang. Protocol of a quantum walk in circuit qed. *Physical Review A*, 100(1):012343, 2019.
- [41] Pranav Gokhale, Jonathan M Baker, Casey Duckering, Natalie C Brown, Kenneth R Brown, and Frederic T Chong. Asymptotic improvements to quantum circuits via qutrits. In *Proceedings of the 46th International Symposium on Computer Architecture*, pages 554–566, 2019.
- [42] Pranav Gokhale, Jonathan M Baker, Casey Duckering, Frederic T Chong, Natalie C Brown, and Kenneth R Brown. Extending the frontier of quantum computers with qutrits. *IEEE Micro*, 40(3):64–72, 2020.
- [43] Ritajit Majumdar, Amit Saha, Amlan Chakrabarti, and Susmita Sur-Kolay. On fault tolerance of circuits with intermediate qutrit-assisted gate decomposition. *arXiv preprint arXiv:2212.07866*, 2022.
- [44] Sreeraman Muralidharan, Chang-Ling Zou, Linshu Li, Jianming Wen, and Liang Jiang. Overcoming erasure errors with multilevel systems. *New Journal of Physics*, 19(1):013026, 2017.
- [45] Earl T Campbell. Enhanced fault-tolerant quantum computing in d-level systems. *Physical review letters*, 113(23):230501, 2014.

- [46] Earl T Campbell, Hussain Anwar, and Dan E Browne. Magic-state distillation in all prime dimensions using quantum reed-muller codes. *Physical Review X*, 2(4):041021, 2012.
- [47] Helle Bechmann-Pasquinucci and Asher Peres. Quantum cryptography with 3-state systems. *Physical Review Letters*, 85(15):3313, 2000.
- [48] Dagmar Bruss and Chiara Macchiavello. Optimal eavesdropping in cryptography with three-dimensional quantum states. *Physical review letters*, 88(12):127901, 2002.
- [49] Alipasha Vaziri, Gregor Weihs, and Anton Zeilinger. Experimental two-photon, three-dimensional entanglement for quantum communication. *Physical review letters*, 89(24):240401, 2002.
- [50] Alexis Morvan, Vinay V Ramasesh, Machiel S Blok, John Mark Kreikebaum, K O’Brien, Larry Chen, Bradley K Mitchell, Ravi K Naik, David I Santiago, and Irfan Siddiqi. Qutrit randomized benchmarking. *Physical review letters*, 126(21):210504, 2021.
- [51] Brendan L Douglas and JB Wang. Efficient quantum circuit implementation of quantum walks. *Physical Review A—Atomic, Molecular, and Optical Physics*, 79(5):052335, 2009.
- [52] Amit Saha, Sudhindu Bikash Mandal, Debasri Saha, and Amlan Chakrabarti. One-dimensional lazy quantum walk in ternary system. *IEEE Transactions on Quantum Engineering*, 2:1–12, 2021.
- [53] Amit Saha, Debasri Saha, and Amlan Chakrabarti. Discrete-time quantum walks in qudit systems. *The European Physical Journal Plus*, 139(11):971, 2024.
- [54] Yale Fan. A generalization of the deutsch-jozsa algorithm to multi-valued quantum logic. In *37th International Symposium on Multiple-Valued Logic (ISMVL’07)*, pages 12–12. IEEE, 2007.
- [55] Alex Bocharov, Shawn X Cui, Martin Roetteler, and Krysta M Svore. Improved quantum ternary arithmetic. *Quantum Information & Computation*, 16(9-10):862–884, 2016.
- [56] Alex Bocharov, Martin Roetteler, and Krysta M Svore. Factoring with qutrits: Shor’s algorithm on ternary and metaplectic quantum architectures. *Physical Review A*, 96(1):012306, 2017.
- [57] Gabriel Bottrill, Mudit Pandey, and Olivia Di Matteo. Exploring the potential of qutrits for quantum optimization of graph coloring. In *2023 IEEE International Conference on Quantum Computing and Engineering (QCE)*, volume 1, pages 177–183. IEEE, 2023.
- [58] Yao-Min Di and Hai-Rui Wei. Synthesis of multi-valued quantum logic circuits by elementary gates. *Physical Review A—Atomic, Molecular, and Optical Physics*, 87(1):012325, 2013.
- [59] Rohit Sarma Sarkar and Bibhas Adhikari. Quantum circuit model for discrete-time three-state quantum walks on cayley graphs. *Phys. Rev. A*, 110:012617, Jul 2024.
- [60] Svyatoslav Kushnarev and Hassan Jameel Asghar. The qudit cirq library: An extension of google’s cirq library for qudits. *arXiv preprint arXiv:2501.07812*, 2025.
- [61] Renato Renner. Security of quantum key distribution. *International Journal of Quantum Information*, 6(01):1–127, 2008.
- [62] Renato Renner, Nicolas Gisin, and Barbara Kraus. Information-theoretic security proof for quantum-key-distribution protocols. *Physical Review A*, 72(1):012332, 2005.
- [63] Feihu Xu, Xiongfeng Ma, Qiang Zhang, Hoi-Kwong Lo, and Jian-Wei Pan. Secure quantum key distribution with realistic devices. *Reviews of modern physics*, 92(2):025002, 2020.
- [64] Marco Tomamichel and Anthony Leverrier. A largely self-contained and complete security proof for quantum key distribution. *Quantum*, 1:14, 2017.
- [65] Jyotirmoy Basak, Arpita Maitra, and Subhamoy Maitra. Device independent quantum key distribution using three-party pseudo-telepathy. In *Progress in Cryptology—INDOCRYPT 2019: 20th International Conference on Cryptology in India, Hyderabad, India, December 15–18, 2019, Proceedings 20*, pages 456–471. Springer, 2019.
- [66] N David Mermin. Simple unified form for the major no-hidden-variables theorems. *Physical review letters*, 65(27):3373, 1990.
- [67] Christopher Portmann and Renato Renner. Security in quantum cryptography. *Reviews of Modern Physics*, 94(2):025008, 2022.
- [68] Nicolas Brunner, Daniel Cavalcanti, Stefano Pironio, Valerio Scarani, and Stephanie Wehner. Bell nonlocality. *Reviews of modern physics*, 86(2):419, 2014.
- [69] Rotem Arnon-Friedman, Frédéric Dupuis, Omar Fawzi, Renato Renner, and Thomas Vidick. Practical device-independent quantum cryptography via entropy accumulation. *Nature communications*, 9(1):459, 2018.
- [70] Asher Peres. *Quantum theory: concepts and methods*, volume 72. Springer, 1997.
- [71] Simon Kochen and Ernst P Specker. The problem of hidden variables in quantum mechanics. *Ernst Specker Selecta*, pages 235–263, 1990.
- [72] Jeffrey Bub. *Interpreting the quantum world*. Cambridge University Press, 1999.
- [73] Jeffrey Bub. Schütte’s tautology and the kochen-specker theorem. *Foundations of Physics*, 26(6):787–806, 1996.
- [74] Michael Kernaghan and Asher Peres. Kochen-specker theorem for eight-dimensional space. *Physics Letters A*, 198(1):1–5, 1995.
- [75] Denis Sych and Gerd Leuchs. A complete basis of generalized bell states. *New Journal of Physics*, 11(1):013006, 2009.
- [76] Ashok Muthukrishnan and Carlos R Stroud Jr. Multivalued logic gates for quantum computation. *Physical review A*, 62(5):052309, 2000.
- [77] Xiongfeng Ma, Xiao Yuan, Zhu Cao, Bing Qi, and Zhen Zhang. Quantum random number generation. *npj Quantum Information*, 2(1):1–9, 2016.
- [78] Nicolas Gisin, André Allan Méthot, and Valerio Scarani. Pseudo-telepathy: input cardinality and bell-type inequalities. *International Journal of Quantum Information*, 5(04):525–534, 2007.

- [79] Costantino Budroni, Adán Cabello, Otfried Gühne, Matthias Kleinmann, and Jan-Åke Larsson. Kochen-specker contextuality. *Reviews of Modern Physics*, 94(4):045007, 2022.
- [80] Samir Kunkri, Guruprasad Kar, Sibasish Ghosh, and Anirban Roy. Winning strategies for pseudo-telepathy games using single non-local box. *Quantum Inf. Comput.*, 7(4):319–328, 2007.
- [81] Renato Renner and Stefan Wolf. Quantum pseudo-telepathy and the kochen-specker theorem. In *International Symposium on Information Theory, 2004. ISIT 2004. Proceedings.*, pages 322–322. IEEE, 2004.
- [82] Jason Zimba and Roger Penrose. On bell non-locality without probabilities: more curious geometry. *Studies in History and Philosophy of Science Part A*, 24(5):697–720, 1993.
- [83] Adán Cabello, Matthias Kleinmann, and Costantino Budroni. Necessary and sufficient condition for quantum state-independent contextuality. *Physical Review Letters*, 114(25):250402, 2015.
- [84] Adán Cabello. Converting contextuality into nonlocality. *Physical Review Letters*, 127(7):070401, 2021.
- [85] Adán Cabello. Bell non-locality and kochen–specker contextuality: how are they connected? *Foundations of Physics*, 51(3):61, 2021.
- [86] Adán Cabello, Simone Severini, and Andreas Winter. Graph-theoretic approach to quantum correlations. *Physical review letters*, 112(4):040401, 2014.
- [87] David A Levin and Yuval Peres. *Markov chains and mixing times*, volume 107. American Mathematical Soc., 2017.
- [88] Hoi-Kwong Lo and Hoi Fung Chau. Unconditional security of quantum key distribution over arbitrarily long distances. *science*, 283(5410):2050–2056, 1999.
- [89] Peter W Shor and John Preskill. Simple proof of security of the bb84 quantum key distribution protocol. *Physical review letters*, 85(2):441, 2000.
- [90] A Robert Calderbank and Peter W Shor. Good quantum error-correcting codes exist. *Physical Review A*, 54(2):1098, 1996.
- [91] Andrew Steane. Multiple-particle interference and quantum error correction. *Proceedings of the Royal Society of London. Series A: Mathematical, Physical and Engineering Sciences*, 452(1954):2551–2577, 1996.
- [92] Toyohiro Tsurumaru. Leftover hashing from quantum error correction: unifying the two approaches to the security proof of quantum key distribution. *IEEE Transactions on Information Theory*, 66(6):3465–3484, 2020.
- [93] Charles H Bennett, Gilles Brassard, and N David Mermin. Quantum cryptography without bell’s theorem. *Physical review letters*, 68(5):557, 1992.
- [94] Ben W Reichardt, Falk Unger, and Umesh Vazirani. A classical leash for a quantum system: Command of quantum systems via rigidity of chsh games. *arXiv preprint arXiv:1209.0448*, 2012.
- [95] Simon Kochen and Ernst P Specker. The problem of hidden variables in quantum mechanics. *Ernst Specker Selecta*, pages 235–263, 1990.
- [96] Charles Ci Wen Lim, Christopher Portmann, Marco Tomamichel, Renato Renner, and Nicolas Gisin. Device-independent quantum key distribution with local bell test. *Physical Review X*, 3(3):031006, 2013.
- [97] Marco Tomamichel and Esther Hänggi. The link between entropic uncertainty and nonlocality. *Journal of Physics A: Mathematical and Theoretical*, 46(5):055301, 2013.
- [98] Gláucia Murta, Federico Grasselli, Hermann Kampermann, and Dagmar Bruß. Quantum conference key agreement: A review. *Advanced Quantum Technologies*, 3(11):2000025, 2020.
- [99] D Marcus Appleby. Symmetric informationally complete–positive operator valued measures and the extended clifford group. *Journal of Mathematical Physics*, 46(5), 2005.

Appendix A: Proof of Theorem IV.2

Proof: In our proposed scheme, the entire protocol operates under the assumption of an ideal, noiseless setting where the communication channel is free from disturbances and the devices used are flawless. However, in practical scenarios, both the channel and the devices are inherently subject to imperfections and noise. Moreover, any adversarial interference is constrained by the laws of quantum physics and would manifest itself in the observed measurement statistics. In the testing phase of our protocol, a noise tolerance parameter η is defined to account for these deviations. Accordingly, each raw key bit generated by Alice and Bob may differ with probability at most η , i.e., for the i -th bit of the raw key, we have $\Pr(K_A^i \neq K_B^i) \leq \eta$. This implies that the probability of agreement on each bit satisfies $\Pr(K_A^i = K_B^i) \geq 1 - \eta$.

Therefore, if Alice and Bob share a k -bit raw key, the probability that their entire raw keys are identical is at least $(1 - \eta)^k$, that is, $\Pr(K_A = K_B) \geq (1 - \eta)^k$. Consequently, the probability that their keys differ is bounded by $\Pr(K_A \neq K_B) < 1 - (1 - \eta)^k$. Setting $\epsilon_{\text{correct}} = 1 - (1 - \eta)^k$, we conclude that the proposed scheme is $\epsilon_{\text{correct}}$ -correct, as required. \square

Appendix B: Proof of Theorem IV.3

Proof: According to the rule of game, both the players start the game with the entangled state $|\psi\rangle := \frac{1}{\sqrt{d}} \sum_{j=0}^{d-1} |j\rangle |j\rangle$. Alice and Bob will measure a random vector v_a and v_b respectively using their measurement basis and will win the game when $v_a = v_b$. Now,

$$\begin{aligned} \Pr(A = v_a, B = v_b) &= |\langle \psi | (|v_a\rangle |v_b\rangle)|^2 \\ &= \left| \frac{1}{\sqrt{d}} \sum_{j=0}^{d-1} \langle j | \langle j | v_a \rangle |v_b\rangle \right|^2 \\ &= \left| \frac{1}{\sqrt{d}} \sum_{j=0}^{d-1} \langle j | v_a \rangle \langle j | v_b \rangle \right|^2 \\ &= \left| \frac{1}{\sqrt{d}} \sum_{j=0}^{d-1} \langle v_a | j \rangle \langle j | v_b \rangle \right|^2 \\ &= \left| \frac{1}{\sqrt{d}} \langle v_a | v_b \rangle \right|^2 \\ &= \begin{cases} \frac{1}{d} & \text{if } v_a = v_b \\ 0 & \text{otherwise} \end{cases} \end{aligned}$$

The winning strategy is thus as follows: Bob measures one of the vectors that is common with Alice, announces the outcome, and Alice subsequently performs her own measurement. Since the measurement basis is orthonormal, the probability that Bob obtains any particular outcome is uniformly distributed among the d basis vectors. The success event can therefore be characterized using the following indicator function defined as

$$\mathbb{1}_X := \begin{cases} 1 & \text{if } X \text{ is true,} \\ 0 & \text{otherwise} \end{cases}$$

the probability of Alice getting a vector v_a , given Bob has measured v_b is thus:

$$\begin{aligned} \Pr(A = v_a | B = v_b) &= \frac{\Pr(A = v_a, B = v_b)}{\Pr(B = v_b)} \\ &= \frac{\frac{1}{d} \cdot \mathbb{1}_{(v_a=v_b)}}{\frac{1}{d}} = \mathbb{1}_{(v_a=v_b)} \end{aligned}$$

Therefore, given the structure of this pseudo-telepathy game, we conclude that, upon a successful round, Alice measures the same vector as Bob with certainty. \square

Appendix C: Proof of Theorem IV.7

Proof: In the proposed scheme, Alice and Bob each input three classical vectors into their respective black-box devices, and in the measurement phase, each outputs a single raw key bit. Accordingly, both the real system (S_{real}) and the ideal system (S_{ideal}) take three classical vectors as input and produce one classical bit as output.

We assume that the random variables $\mathbf{X}_{\text{ideal}}$ and \mathbf{X}_{real} represent the outcomes of the ideal and real systems, respectively, when calculating the closeness measure in terms of statistical distance. The two random variables

are defined over the set $S = \{0, 1\}$. The statistical distance between these two random variables will be as follows.

$$\begin{aligned}
& \frac{1}{2} \sum_{x \in S} |Pr(\mathbf{X}_{\text{ideal}} = x) - Pr(\mathbf{X}_{\text{real}} = x)| \\
&= \frac{1}{2} (|Pr(\mathbf{X}_{\text{ideal}} = 0) - Pr(\mathbf{X}_{\text{real}} = 0)| \\
&\quad + |Pr(\mathbf{X}_{\text{ideal}} = 1) - Pr(\mathbf{X}_{\text{real}} = 1)|) \\
&= \frac{1}{2} (|\frac{1}{2} - (\frac{1}{2} - \eta)| + |\frac{1}{2} - (\frac{1}{2} - \eta)|) \\
&= \eta
\end{aligned}$$

This concludes the proof. \square

Appendix D: Proof of Theorem IV.8

Proof: The proof follows from the discussion in Section IV D., Equation 6. As we know, in our protocol, the set Γ depends on the error rate η and is characterized by the condition

$$(\langle v_B | \otimes \langle v_A |) \sigma_{AB} (|v_A\rangle \otimes |v_B\rangle) \leq \frac{\eta}{2},$$

for all v_A and v_B denote the measurement bases of Alice and Bob, respectively, such that $v_B \neq v_\ell$ and

$$v_A \neq \begin{cases} v_1, & \text{if } v_1 = v_\ell, \\ v_2, & \text{otherwise.} \end{cases}$$

We now define a completely positive map (CPM) [61] \mathcal{D} as

$$\mathcal{D}(\sigma_{AB}) := \frac{1}{9} \sum_{\tau \in GP} \tau^{\otimes 2} \sigma_{AB} \tau^{\otimes 2},$$

where GP denotes Sylvester's generalized Pauli matrices [99]:

$$GP = \left\{ (\Sigma_1)^k (\Sigma_2)^j \right\}_{k,j=1}^3,$$

with

$$\Sigma_1 := \begin{bmatrix} 0 & 0 & 1 \\ 1 & 0 & 0 \\ 0 & 1 & 0 \end{bmatrix}, \quad \Sigma_2 := \begin{bmatrix} 1 & 0 & 0 \\ 0 & \omega & 0 \\ 0 & 0 & \omega^2 \end{bmatrix}, \quad \text{where } 1 + \omega + \omega^2 = 0.$$

Let $\tilde{\sigma}_{AB} := \mathcal{D}(\sigma_{AB})$, and let $\tilde{\sigma}_{ABE}$ be the arbitrary purification of $\tilde{\sigma}_{AB}$, which includes interference from Eve. We define

$$\tilde{\sigma}_{XYE} = (\mathcal{E}_{XY \leftarrow AB}^{\text{Meas}} \otimes I_{|E|}) \tilde{\sigma}_{ABE}.$$

where $\mathcal{E}_{XY \leftarrow AB}^{\text{Meas}} : \mathcal{H}_A \otimes \mathcal{H}_B \rightarrow \mathcal{H}_X \otimes \mathcal{H}_Y$ denote the measurement map, where, following the measurement in a chosen basis by Alice and Bob, the Hilbert spaces \mathcal{H}_A and \mathcal{H}_B are transformed into the Hilbert spaces \mathcal{H}_X and \mathcal{H}_Y , respectively.

It is trivial to see that

$$\tilde{\sigma}_{AB} = \sum_{i=0}^8 \lambda_i |\varphi_i\rangle \langle \varphi_i|,$$

where $\{|\varphi_i\rangle\}_{i=0}^8$ are the 3-dimensional Bell basis (mentioned in Section III C), denoted as:

$$\begin{aligned}
|\varphi_0\rangle &= \frac{|00\rangle + |11\rangle + |22\rangle}{\sqrt{3}}, \\
|\varphi_1\rangle &= \frac{|00\rangle + \omega |11\rangle + \omega^2 |22\rangle}{\sqrt{3}}, \\
|\varphi_2\rangle &= \frac{|00\rangle + \omega^2 |11\rangle + \omega |22\rangle}{\sqrt{3}}, \\
|\varphi_3\rangle &= \frac{|01\rangle + |12\rangle + |20\rangle}{\sqrt{3}}, \\
|\varphi_4\rangle &= \frac{|01\rangle + \omega |12\rangle + \omega^2 |20\rangle}{\sqrt{3}}, \\
|\varphi_5\rangle &= \frac{|01\rangle + \omega^2 |12\rangle + \omega |20\rangle}{\sqrt{3}}, \\
|\varphi_6\rangle &= \frac{|02\rangle + |10\rangle + |21\rangle}{\sqrt{3}}, \\
|\varphi_7\rangle &= \frac{|02\rangle + \omega |10\rangle + \omega^2 |21\rangle}{\sqrt{3}}, \\
|\varphi_8\rangle &= \frac{|02\rangle + \omega^2 |10\rangle + \omega |21\rangle}{\sqrt{3}}.
\end{aligned}$$

In other words, $\tilde{\sigma}_{AB}$ is a diagonal matrix with respect to the Bell basis. Further, since \mathcal{D} commutes with the measurement operation on $\mathcal{H}_A \otimes \mathcal{H}_B$, it is straightforward to confirm that the conditional entropy $H(X|Y)$ for σ_{XY} is bounded above by the corresponding entropy for $\tilde{\sigma}_{XY}$. Similarly, because $\tilde{\sigma}_{ABE}$ is a purification of $\tilde{\sigma}_{AB}$, the conditional entropy $H(X|E)$ for σ_{XE} is bounded below by the entropy of $\tilde{\sigma}_{XE}$. Therefore, it is sufficient to establish that the inequality in the lemma holds for the operator $\tilde{\sigma}_{XYE}$, which is derived from the diagonal operator $\tilde{\sigma}_{AB}$.

Let $|e_i\rangle$ be the orthonormal basis Eve uses to interfere with Alice and Bob's communication. Then

$$\tilde{\sigma}_{XYE} = |\Psi\rangle\langle\Psi| \in \mathcal{P}(\mathcal{H}_A \otimes \mathcal{H}_B \otimes \mathcal{H}_E),$$

with $|\Psi\rangle$ defined as:

$$|\Psi\rangle = \sum_{i=0}^8 \sqrt{\lambda_i} |\varphi_i\rangle_{AB} \otimes |e_i\rangle_E.$$

We define

$$|f_{x,y}\rangle = \sum_{j=0}^2 \omega^{jx} \sqrt{\frac{\lambda_{3(y\oplus x)+j}}{3}} |e_{3(y\oplus x)+j}\rangle$$

where $a \oplus b := (a + b) \bmod 3$ and $x, y \in \{0, 1, 2\}$. With $\omega \in \mathbb{C}$ such that $\omega^3 = 1$ and $1 + \omega + \omega^2 = 0$, each of the states of f are as follows:

1. $|f_{00}\rangle = \sqrt{\frac{\lambda_0}{3}} |e_0\rangle + \sqrt{\frac{\lambda_1}{3}} |e_1\rangle + \sqrt{\frac{\lambda_2}{3}} |e_2\rangle$
2. $|f_{01}\rangle = \sqrt{\frac{\lambda_3}{3}} |e_3\rangle + \sqrt{\frac{\lambda_4}{3}} |e_4\rangle + \sqrt{\frac{\lambda_5}{3}} |e_5\rangle$
3. $|f_{02}\rangle = \sqrt{\frac{\lambda_6}{3}} |e_6\rangle + \sqrt{\frac{\lambda_7}{3}} |e_7\rangle + \sqrt{\frac{\lambda_8}{3}} |e_8\rangle$
4. $|f_{10}\rangle = \sqrt{\frac{\lambda_6}{3}} |e_6\rangle + \omega \sqrt{\frac{\lambda_7}{3}} |e_7\rangle + \omega^2 \sqrt{\frac{\lambda_8}{3}} |e_8\rangle$

5. $|f_{11}\rangle = \sqrt{\frac{\lambda_0}{3}} |e_0\rangle + \omega \sqrt{\frac{\lambda_1}{3}} |e_1\rangle + \omega^2 \sqrt{\frac{\lambda_2}{3}} |e_2\rangle$
6. $|f_{12}\rangle = \sqrt{\frac{\lambda_3}{3}} |e_3\rangle + \omega \sqrt{\frac{\lambda_4}{3}} |e_4\rangle + \omega^2 \sqrt{\frac{\lambda_5}{3}} |e_5\rangle$
7. $|f_{20}\rangle = \sqrt{\frac{\lambda_3}{3}} |e_3\rangle + \omega^2 \sqrt{\frac{\lambda_4}{3}} |e_4\rangle + \omega \sqrt{\frac{\lambda_5}{3}} |e_5\rangle$
8. $|f_{21}\rangle = \sqrt{\frac{\lambda_6}{3}} |e_6\rangle + \omega^2 \sqrt{\frac{\lambda_7}{3}} |e_7\rangle + \omega \sqrt{\frac{\lambda_8}{3}} |e_8\rangle$
9. $|f_{22}\rangle = \sqrt{\frac{\lambda_0}{3}} |e_0\rangle + \omega^2 \sqrt{\frac{\lambda_1}{3}} |e_1\rangle + \omega \sqrt{\frac{\lambda_2}{3}} |e_2\rangle$

We can restate $|\Psi\rangle$ as:

$$|\Psi\rangle = \sum_{x,y \in \{0,1,2\}} |x\rangle \otimes |y\rangle \otimes |f_{x,y}\rangle.$$

We infer that

$$\tilde{\sigma}_{XYE} = \sum_{x,y} |x\rangle \langle x| \otimes |y\rangle \langle y| \otimes |f_{x,y}\rangle \langle f_{x,y}|,$$

because the operator $\tilde{\sigma}_{XYE}$ is obtained from $\tilde{\sigma}_{ABE}$ by orthonormal measurements on \mathcal{H}_A and \mathcal{H}_B .

Now, to calculate the key rate, we can calculate the following values: i) $H(X|E) \approx H(\tilde{\sigma}_{XE}) - H(\tilde{\sigma}_E)$ and ii) $H(X|Y) \approx H(\tilde{\sigma}_{XY}) - H(\tilde{\sigma}_Y)$, where if ρ is a density matrix with eigenvalues $\{a_i\}_{i=1}^n$, then

$$H(\rho) = -\text{Tr}(\rho \log_3 \rho) = -\sum a_i \log_3 a_i,$$

with the base of the logarithm set to 3, as we are working with qutrits.

Now, to compute these values, we use partial traces to collapse one of the dimensions. In particular,

$$\begin{aligned} \tilde{\sigma}_{XE} &= \sum_{y=0}^2 (I_3 \otimes \langle y| \otimes I_9) \tilde{\sigma}_{XYE} (I_3 \otimes |y\rangle \otimes I_9) \\ &= \sum_{y'} (I_3 \otimes \langle y'| \otimes I_9) \left(\sum_{x,y} |x\rangle \langle x| \otimes |y\rangle \langle y| \otimes |f_{x,y}\rangle \langle f_{x,y}| \right) (I_3 \otimes |y'\rangle \otimes I_9) \\ &= \sum_{x,y,y'} |x\rangle \langle x| \otimes |\langle y'|y\rangle|^2 \otimes |f_{x,y}\rangle \langle f_{x,y}| \\ &= \sum_{x,y,y'} |x\rangle \langle x| \otimes \mathbb{1}_{(y'=y)} \otimes |f_{x,y}\rangle \langle f_{x,y}| \quad [\mathbb{1}_X \text{ as stated in B}] \\ &= \sum_x |x\rangle \langle x| \otimes \left(\sum_y |f_{x,y}\rangle \langle f_{x,y}| \right). \end{aligned}$$

Similarly, it can be shown that

$$\tilde{\sigma}_E = \sum_{x,y} |f_{x,y}\rangle \langle f_{x,y}|$$

Before calculating the entropies as stated above, we first present the matrix form of the corresponding density states. First, we define a sequence of matrices $B_i^{(j)}$ as follows: For $i, j \in \mathbb{Z}_3$

$$B_i^{(j)} := \frac{1}{3} \begin{bmatrix} \lambda_{3i} & \omega^{2j} \sqrt{\lambda_{3i} \lambda_{3i+1}} & \omega^j \sqrt{\lambda_{3i} \lambda_{3i+2}} \\ \omega^j \sqrt{\lambda_{3i} \lambda_{3i+1}} & \lambda_{3i+1} & \omega^{2j} \sqrt{\lambda_{3i+1} \lambda_{3i+2}} \\ \omega^{2j} \sqrt{\lambda_{3i} \lambda_{3i+2}} & \omega^{2j} \sqrt{\lambda_{3i+1} \lambda_{3i+2}} & \lambda_{3i+2} \end{bmatrix}$$

Note that all nine matrices have a determinant of zero, implying at least one of their three eigenvalues is 0. The sum of the eigenvalues for an index i is $\frac{\lambda_{3i} + \lambda_{3i+1} + \lambda_{3i+2}}{3}$, and testing it confirms that one of the eigenvalues is $\frac{\lambda_{3i} + \lambda_{3i+1} + \lambda_{3i+2}}{3}$. This leaves us with the matrix $B_i^{(j)}$ having eigenvalues $\frac{\lambda_{3i} + \lambda_{3i+1} + \lambda_{3i+2}}{3}$ with multiplicity 1 and 0 with multiplicity 2. Now we define a block diagonal matrix

$$B^{(j)} := \left[\begin{array}{c|c|c} B_0^{(j)} & 0_{3 \times 3} & 0_{3 \times 3} \\ \hline 0_{3 \times 3} & B_1^{(j)} & 0_{3 \times 3} \\ \hline 0_{3 \times 3} & 0_{3 \times 3} & B_2^{(j)} \end{array} \right]$$

Then $\tilde{\sigma}_{XE}$ has the matrix form:

$$\left[\begin{array}{c|c|c} B^{(0)} & 0_{9 \times 9} & 0_{9 \times 9} \\ \hline 0_{9 \times 9} & B^{(1)} & 0_{9 \times 9} \\ \hline 0_{9 \times 9} & 0_{9 \times 9} & B^{(2)} \end{array} \right]$$

Since this matrix is a block diagonal matrix consisting of 9 matrices, the eigenvalues of this block matrix are the list of all eigenvalues of these 9 matrices. So the eigenvalues of $\tilde{\sigma}_{XE}$ are: 0 with multiplicity 18, $\frac{\lambda_0 + \lambda_1 + \lambda_2}{3}$ with multiplicity 3, $\frac{\lambda_3 + \lambda_4 + \lambda_5}{3}$ with multiplicity 3, and $\frac{\lambda_6 + \lambda_7 + \lambda_8}{3}$ with multiplicity 3. Using the fact that $0 \log 0 := 0$, we have

$$\begin{aligned} H(\tilde{\sigma}_{XE}) &= -3 \left(\frac{\lambda_0 + \lambda_1 + \lambda_2}{3} \log_3 \left(\frac{\lambda_0 + \lambda_1 + \lambda_2}{3} \right) + \frac{\lambda_3 + \lambda_4 + \lambda_5}{3} \log_3 \left(\frac{\lambda_3 + \lambda_4 + \lambda_5}{3} \right) \right. \\ &\quad \left. + \frac{\lambda_6 + \lambda_7 + \lambda_8}{3} \log_3 \left(\frac{\lambda_6 + \lambda_7 + \lambda_8}{3} \right) \right) \\ &= (\lambda_0 + \lambda_1 + \dots + \lambda_8) - (\lambda_0 + \lambda_1 + \lambda_2) \log_3(\lambda_0 + \lambda_1 + \lambda_2) \\ &\quad - (\lambda_3 + \lambda_4 + \lambda_5) \log_3(\lambda_3 + \lambda_4 + \lambda_5) - (\lambda_6 + \lambda_7 + \lambda_8) \log_3(\lambda_6 + \lambda_7 + \lambda_8) \\ &= 1 - (\lambda_0 + \lambda_1 + \lambda_2) \log_3(\lambda_0 + \lambda_1 + \lambda_2) - (\lambda_3 + \lambda_4 + \lambda_5) \log_3(\lambda_3 + \lambda_4 + \lambda_5) \\ &\quad - (\lambda_6 + \lambda_7 + \lambda_8) \log_3(\lambda_6 + \lambda_7 + \lambda_8) \end{aligned}$$

Similarly, $\tilde{\sigma}_E$ has the diagonal matrix form of a diagonal matrix: $\text{diag}(\lambda_0, \lambda_1, \dots, \lambda_8)$. So $H(\tilde{\sigma}_E) = -\sum_{i=0}^8 \lambda_i \log_3(\lambda_i)$

At last we come to the analysis of $H(X|Y) = H(\tilde{\sigma}_{XY}) - H(\tilde{\sigma}_Y)$. $\tilde{\sigma}_{XY}$ has the form

$$\frac{1}{3} \left[\begin{array}{cccccccc} \lambda_0^2 + \lambda_1^2 + \lambda_2^2 & 0 & 0 & 0 & 0 & 0 & 0 & 0 \\ 0 & \lambda_3^2 + \lambda_4^2 + \lambda_5^2 & 0 & 0 & 0 & 0 & 0 & 0 \\ 0 & 0 & \lambda_6^2 + \lambda_7^2 + \lambda_8^2 & 0 & 0 & 0 & 0 & 0 \\ 0 & 0 & 0 & \lambda_6^2 + \lambda_7^2 + \lambda_8^2 & 0 & 0 & 0 & 0 \\ 0 & 0 & 0 & 0 & \lambda_0^2 + \lambda_1^2 + \lambda_2^2 & 0 & 0 & 0 \\ 0 & 0 & 0 & 0 & 0 & \lambda_3^2 + \lambda_4^2 + \lambda_5^2 & 0 & 0 \\ 0 & 0 & 0 & 0 & 0 & 0 & \lambda_3^2 + \lambda_4^2 + \lambda_5^2 & 0 \\ 0 & 0 & 0 & 0 & 0 & 0 & 0 & \lambda_6^2 + \lambda_7^2 + \lambda_8^2 \\ 0 & 0 & 0 & 0 & 0 & 0 & 0 & 0 & \lambda_0^2 + \lambda_1^2 + \lambda_2^2 \end{array} \right]$$

and $\tilde{\sigma}_Y$ has the form

$$\frac{1}{3} \left[\begin{array}{ccc} \lambda_0^2 + \lambda_1^2 + \dots + \lambda_8^2 & & \\ & \lambda_0^2 + \lambda_1^2 + \dots + \lambda_8^2 & \\ & & \lambda_0^2 + \lambda_1^2 + \dots + \lambda_8^2 \end{array} \right] = \frac{1}{3} \cdot I$$

So $\tilde{\sigma}_{XY}$ has 3 distinct eigenvalues $\frac{\lambda_0^2 + \lambda_1^2 + \lambda_2^2}{3}$, $\frac{\lambda_3^2 + \lambda_4^2 + \lambda_5^2}{3}$ and $\frac{\lambda_6^2 + \lambda_7^2 + \lambda_8^2}{3}$, each with multiplicity 3,

while $\tilde{\sigma}_Y$ has a single eigenvalue $\frac{1}{3}$ with multiplicity 3. So

$$\begin{aligned}
H(\tilde{\sigma}_{XY}) &= -3 \left(\frac{\lambda_0^2 + \lambda_1^2 + \lambda_2^2}{3} \log_3 \left(\frac{\lambda_0^2 + \lambda_1^2 + \lambda_2^2}{3} \right) + \frac{\lambda_3^2 + \lambda_4^2 + \lambda_5^2}{3} \log_3 \left(\frac{\lambda_3^2 + \lambda_4^2 + \lambda_5^2}{3} \right) \right. \\
&\quad \left. + \frac{\lambda_6^2 + \lambda_7^2 + \lambda_8^2}{3} \log_3 \left(\frac{\lambda_6^2 + \lambda_7^2 + \lambda_8^2}{3} \right) \right) \\
&= (\lambda_0^2 + \lambda_1^2 + \dots + \lambda_8^2) - (\lambda_0^2 + \lambda_1^2 + \lambda_2^2) \log_3(\lambda_0^2 + \lambda_1^2 + \lambda_2^2) \\
&\quad - (\lambda_3^2 + \lambda_4^2 + \lambda_5^2) \log_3(\lambda_3^2 + \lambda_4^2 + \lambda_5^2) - (\lambda_6^2 + \lambda_7^2 + \lambda_8^2) \log_3(\lambda_6^2 + \lambda_7^2 + \lambda_8^2) \\
&= 1 - (\lambda_0^2 + \lambda_1^2 + \lambda_2^2) \log_3(\lambda_0^2 + \lambda_1^2 + \lambda_2^2) - (\lambda_3^2 + \lambda_4^2 + \lambda_5^2) \log_3(\lambda_3^2 + \lambda_4^2 + \lambda_5^2) \\
&\quad - (\lambda_6^2 + \lambda_7^2 + \lambda_8^2) \log_3(\lambda_6^2 + \lambda_7^2 + \lambda_8^2)
\end{aligned}$$

and

$$H(\tilde{\sigma}_Y) = -3 \left(\frac{1}{3} \log_3 \frac{1}{3} \right) = 1$$

So in the end, we get,

$$\begin{aligned}
\text{Key rate} &\geq H(X|E) - H(X|Y) = H(\tilde{\sigma}_{XE}) - H(\tilde{\sigma}_E) - H(\tilde{\sigma}_{XY}) + H(\tilde{\sigma}_Y) \\
&= 1 - (\lambda_0 + \lambda_1 + \lambda_2) \log_3(\lambda_0 + \lambda_1 + \lambda_2) - (\lambda_3 + \lambda_4 + \lambda_5) \log_3(\lambda_3 + \lambda_4 + \lambda_5) \\
&\quad - (\lambda_6 + \lambda_7 + \lambda_8) \log_3(\lambda_6 + \lambda_7 + \lambda_8) + (\lambda_0^2 + \lambda_1^2 + \lambda_2^2) \log_3(\lambda_0^2 + \lambda_1^2 + \lambda_2^2) \\
&\quad + (\lambda_3^2 + \lambda_4^2 + \lambda_5^2) \log_3(\lambda_3^2 + \lambda_4^2 + \lambda_5^2) - (\lambda_6^2 + \lambda_7^2 + \lambda_8^2) \log_3(\lambda_6^2 + \lambda_7^2 + \lambda_8^2) \\
&\quad + \sum_{i=0}^8 \lambda_i \log_3(\lambda_i)
\end{aligned}$$

The rest of the proof follows immediately. □
